Log-periodic route to fractal functions

S. Gluzman[1] and D. Sornette[1,2,3]

[1]Institute of Geophysics and Planetary Physics, University of California Los Angeles, Los Angeles, California 90095-1567

[2]Department of Earth and Space Sciences, UCLA, Box 951567, Los Angeles, California 90095-1567

[3]Laboratoire de Physique de la Matière Condensée, CNRS UMR 6622 and Université de Nice-Sophia Antipolis, 06108 Nice Cedex 2, France

(Received 27 June 2001; revised manuscript received 5 December 2001; published 7 March 2002)

Log-periodic oscillations have been found to decorate the usual power-law behavior found to describe the approach to a critical point, when the continuous scale-invariance symmetry is partially broken into a discrete-scale invariance symmetry. For Ising or Potts spins with ferromagnetic interactions on hierarchical systems, the relative magnitude of the log-periodic corrections are usually very small, of order 10^{-5}. In growth processes [diffusion limited aggregation (DLA)], rupture, earthquake, and financial crashes, log-periodic oscillations with amplitudes of the order of 10% have been reported. We suggest a "technical" explanation for this 4 order-of-magnitude difference based on the property of the "regular function" $g(x)$ embodying the effect of the microscopic degrees of freedom summed over in a renormalization group (RG) approach $F(x)=g(x)+\mu^{-1}F(\gamma x)$ of an observable F as a function of a control parameter x. For systems for which the RG equation has not been derived, the previous equation can be understood as a Jackson q integral, which is the natural tool for describing discrete-scale invariance. We classify the "Weierstrass-type" solutions of the RG into two classes characterized by the amplitudes A_n of the power-law series expansion. These two classes are separated by a novel "critical" point. Growth processes (DLA), rupture, earthquake, and financial crashes thus seem to be characterized by oscillatory or bounded regular microscopic functions that lead to a slow power-law decay of A_n, giving strong log-periodic amplitudes. If in addition, the phases of A_n are ergodic and mixing, the observable presents self-affine nondifferentiable properties. In contrast, the regular function of statistical physics models with "ferromagnetic"-type interactions at equibrium involves unbound logarithms of polynomials of the control variable that lead to a fast exponential decay of A_n giving weak log-periodic amplitudes and smoothed observables.

DOI: 10.1103/PhysRevE.65.036142 PACS number(s): 05.70.Jk, 47.53.+n

I. INTRODUCTION

The existence of log-periodic oscillatory corrections to the power-laws associated with critical phenomena and, more generally, to observables of systems endowed with the scale-invariance symmetry has been recognized since the 1960s (see [1] for a recent review and references therein). The log-periodic oscillations result from a partial breakdown of the continuous scale-invariance symmetry into a discrete-scale-invariance symmetry, as occurs for instance in hierarchical lattices.

However, for one of the most studied class of models exhibiting these oscillations, i.e., Potts model with ferromagnetic interactions on hierarchical lattices, the relative magnitude of the log-periodic corrections are usually very small, of order 10^{-5} [2]. In contrast, in growth processes [diffusion limited aggregation (DLA)] [3,4], rupture [5], earthquakes [6], and financial crashes [7,8] amplitudes of the order of 10% have been reported.

Here, we propose an explanation for this puzzling observation of an 4 order-of-magnitude difference based on the nature of the microscopic interactions of the systems. Within a renormalization group (RG) approach, an observable at one scale can be related by a functional relation to the same observable at another scale, with the addition of the contribution of the degrees of freedom left over by the procedure of decimation or of change of scale. This contribution is called the "regular part" of the renormalization group equation of the observable. For systems for which the RG equation has not been derived, the RG equation can be understood without reference to the RG as a Jackson q integral [9], which is the natural tool [10,11] for describing discrete-scale invariance. Here, we do not discuss the mechanisms by which the continuous scale-invariance symmetry is broken to give discrete-scale invariance but rather present a phenomenological approach based on the functional RG/Jackson q-integral equation.

Using the Mellin transform applied to the formal series solution of the renormalization group, we identify two broad classes of systems based on the nature of the decay with order n of the amplitudes A_n of the power-law series expansion of the observable:

(1) Systems with quasiperiodic "regular part" and/or with compact support have coefficients A_n decaying as a power law $A_n \sim n^{-p}$, leading to strong log-periodic oscillatory amplitudes; if in addition, the phases of A_n are ergodic and mixing, the observable presents singular properties everywhere, similar to those of 'Weierstrass-type" functions.

(2) Systems with nonperiodic "regular part" with unbound support have A_n decaying as an exponential $A_n \sim e^{-\kappa n}$ of their order n, leading to exceedingly small log-periodic oscillatory amplitudes and regular smooth observables.

We find families of "regular parts" that belong to both classes, with a "critical" transition from the first to the other as a parameter is varied.

TABLE I. Synthesis of the different classes of Weierstrass-type functions according to the general classification (21), $A_n \sim (1/n^p) e^{-\kappa n} e^{i\psi_n}$ of the expansion (18) in terms of a series of power laws x^{-s_n}. The parameters p, $\kappa \geqslant 0$, and ψ_n are determined by the form of $g(x)$ and the values of μ and γ. All numerical values given in this table correspond to $m=0.5, \omega=7.7$ corresponding to $\gamma=2.26$ and $\mu=\sqrt{\gamma}=1.5$. The last two columns quantify the amplitude of the log-periodic oscillations with respect to the leading real power law.

$g(x)$	p	κ	ψ_n	$\lvert A_{n=1}/A_{n=0}\rvert$	$\lvert A_{n=2}/A_{n=0}\rvert$
$\cos(x)$	$m+1/2$	0	$\omega n \ln(\omega n)$	0.065	0.032
$\exp(-x)$	$m+1/2$	$(\pi/2)\omega$	$\omega n \ln(\omega n)$	5.12×10^{-7}	1.432×10^{-12}
$\exp[-cx]\cos(xs)$[a]	$m+1/2$	$([\pi/2]-\alpha)\omega$	$\omega n \ln(\omega n)$		
$(1+x^2)^{-1}$	0	$(\pi/2)\omega$	$(\pi/2)m$	9.901×10^{-6}	4.414×10^{-11}
$\log(1+x)$	1	$\pi\omega$	$-\pi m$	4.045×10^{-12}	≈ 0
$\exp(-x^h)$	$m/h+1/2$	$(\pi/2h)\omega$	$[(\omega n)/h]\ln(\omega n)$	0.064 ($h=50$)	0.03 ($h=50$)
				4.386×10^{-4} ($h=2$)	6.177×10^{-7} ($h=2$)
$\sin(x)/x^\delta$	$m+\delta+1/2$	0	$-\omega n \ln(\omega n)$	0.044 ($\delta=0.1$)	0.021 ($\delta=0.1$)
				0.091 ($\delta=-0.1$)	0.049 ($\delta=-0.1$)
$\mathrm{Si}(x)$	$m+3/2$	0	$\omega n \ln(\omega n)$	4.199×10^{-3}	1.053×10^{-3}
$1-x^h$ $0<x<1$	2	0	π	0.064 ($h=50$)	0.031 ($h=50$)
				0.012 ($h=2$)	3.146×10^{-3} ($h=2$)

[a] $c=\cos\alpha$ and $s=\sin\alpha$.

A known example of a system of the first class is the q-state Potts model with *antiferromagnetic* interactions [12,13]. Another example is the statistics of closed-loop self-avoiding walks per site on a family of regular fractals with a discrete-scale-invariant geometry such as the Sieirpinsky gasket [14]. A known example of the second class is the q-state Potts model with *ferromagnetic* interactions [2].

Section II introduces the renormalization group with a single control parameter, its formal solution with the presence of log-periodic corrections associated with discrete-scale invariance. Section III uses the Mellin transform to resum the formal series solution of the renormalization group into a power-law series. Section IV presents the general classification within the two classes alluded to above in terms of the leading exponential or power-law decay of the coefficients of this power-law expansion. It examines the conditions under which the observable can develop nondifferentiable fractal properties similar to Weierstrass-type functions. A family of ''regular parts'' is introduced that exhibits a critical transition between the two classes. Section V presents many more examples of both classes. Section VI concludes. Table I offers a synthesis of the classification in terms of the decay of the coefficients A_n of the power series expansion of the observable for various choices of the ''regular part'' of the renormalization group.

II. "WEIERSTRASS-TYPE FUNCTIONS" FROM DISCRETE RENORMALIZATION GROUP EQUATIONS

Speaking about a material shape, a mathematical object or function, the symmetry of scale invariance refers to their invariance with respect to changes of scales of observation (see [15,16] for general introductions). In a nutshell, scale invariance simply means reproducing itself on different time or space scales. Specifically, an observable f that depends on a ''control'' parameter x is scale invariant under the arbitrary change $x \to \gamma x$ if there is a number $\mu(\gamma)$ such that

$$f(x)=\frac{1}{\mu} f(\gamma x). \tag{1}$$

Such scale invariance occurs for instance at the critical points $t=t_c$ of systems exhibiting a continuous phase transition. The renormalization group theory has been developed to provide an understanding of the emergence of the self-similar property (1) from a systematic scale change and spin decimation procedure [17].

Calling K the coupling (e.g., $K=e^{J/T}$ for a spin model where J is interaction coefficient and T is the temperature) and R the renormalization group map between two successive magnification steps, the free energy f per lattice site, bond, atom or element obeys the self-consistent equation,

$$f(K)=g(K)+\frac{1}{\mu} f[R(K)], \tag{2}$$

where g is a regular part that is made of the free energy of the degrees of freedom summed over two successive renormalizations, $\mu>1$ is the ratio of the number of degrees of freedom between two successive renormalizations. In general, this relationship (2) is an approximation whose validity requires the study of the impact of many-body interactions. When these higher-order interactions can be considered secondary as the scale of description increases (corresponding to so-called ''irrelevant'' operators), expression (2) becomes asymptotically exact at large scales. For perfectly self-similar problems, for instance, for physical systems with nearest-neighbor interactions defined on regular geometrical fractals such as the Cantor set, the Sierpinsky Gasket, etc., or on regular hierarchical lattices, expression (2) is exact at all scales.

It is solved recursively by

$$f(K)=\sum_{n=0}^{\infty} \frac{1}{\mu^n} g[R^{(n)}(K)], \tag{3}$$

where $R^{(n)}$ is the nth iterate of the renormalization transformation. Around fixed points $R(K_c)=K_c$, the renormalization group map can be expanded up to first order in $K-K_c$ as $R(K)=\gamma(K-K_c)$. Posing $x=K-K_c$, we have $R^{(n)}(x)=\gamma^n x$ and the solution (3) becomes

$$f(x)=\sum_{n=0}^{\infty}\frac{1}{\mu^n}g[\gamma^n x]. \tag{4}$$

In principle, Eq. (4) is only applicable sufficiently ''close'' to the critical point $x=0$, that the higher-order terms in the expansion $R(K)=\gamma(K-K_c)$ can be neglected. The effect of nonlinear corrections terms for $R(K)$ have been considered in [2,12].

The form (3) or (4) has not been derived from first principles for growth, rupture, and other out-of-equilibrium processes alluded to above, even if there are various attempts to develop approximate RG descriptions on specific models of these processes. It may thus seem a little premature to use this discrete renormalization group description for these systems. Actually, expression (4) can be obtained without any reference to a renormalization group approach: as soon as the system exhibits a discrete-scale invariance, the natural tool is provided by q derivatives [11] from which it is seen that expression (4) is nothing but a Jackson q integral [9] of the function $g(x)$, which constitutes the natural generalization of regular integrals for discretely self-similar systems [11]. The way the Jackson q integral is related to the free energy of a spin system on a hierarchical lattice was explained in [18].

In the mathematical literature, the function (4) is called a *Weierstrass-type function*, to refer to the introduction by Weierstrass of the function [19]

$$f_W=\sum_{n=0}^{\infty}b^n\cos[a^n\pi x], \tag{5}$$

corresponding to the special case $\mu=1/b$, $\gamma=a$, and $g(x)=\cos[\pi x]$. To the surprise of mathematicians of the 19th century, Weierstrass showed that the function (5) is continuous but differentiable nowhere, provided $0<b<1, a>1$, and $ab>1+\frac{2}{3}\pi$. Note that, in the context of the renormalization group of critical phenomena, the condition $a=\gamma>1$ implies that the fixed point K_c is unstable. Hardy was able to improve later on the last bound and obtain that the Weierstrass function (5) is nondifferentiable everywhere as soon as $ab>1$ [20]. In addition, Hardy showed that it satisfies the following Lipschitz condition (corresponding to self-affine scaling) for $ab>1$, which is much more than just the statement of nondifferentiability,

$$f_W(x+h)-f_W(x)\sim|h|^m, \quad \text{for all } x \quad \text{where}$$
$$m=\ln[1/b]/\ln a. \tag{6}$$

Note that for $ab>1$, $m<1$, expression (6) shows that $f_W(x+h)-f_W(x)\gg|h|$ for $h\to 0$. As a consequence, the ratio $[f_W(x+h)-f_W(x)]/h$ has no limit that recovers the property of nondifferentiability. Continuity is obvious from the fact that $f_W(x+h)-f_W(x)\to 0$ as $h\to 0$ since $m>0$. For the border case $a=b$ discovered by Cellerier before 1850, f_W is not nondifferentiable in a strict sense since it possesses infinite differential coefficients at an everywhere dense set of points [21]. Richardson is credited with the first mention of the potential usefulness for the description of the nature of the continuous-everywhere nondifferentiable Weierstrass function [22]. Shlesinger and co-workers [23] have previously noticed and studied the correspondence between Eq. (4) and the Weierstrass function.

If one is interested in the nonregular (or nonanalytic) behavior only close to the critical point $x=0$, the regular part can be dropped and the analysis of Eq. (1) is sufficient. It is then easy to show that the most general solution of Eq. (1) is (see [1] and references therein)

$$f(x)=x^m\ P\left(\frac{\ln x}{\ln\gamma}\right), \tag{7}$$

where

$$m=\frac{\ln\mu}{\ln\gamma}, \tag{8}$$

and $P(y)$ is an arbitrary periodic function of its argument y of period 1. Its specification is actually determined by the regular part $g(x)$ of the renormalization group equation, as shown for instance in the explicit solution (4). The scaling law $f(x)\sim x^m$ implied by Eq. (7) is a special case of Eq. (6) obtained by putting $x=0$ and replacing h by x in Eq. (6).

The Laplace transform $f_L(\beta)$ of $f(x)$ defined by Eq. (4) also obeys a renormalization equation of the type (2). Denoting $g_L(\beta)$, the Laplace transform of the regular part $g(x)$, we have

$$f_L(\beta)=\sum_{n=0}^{\infty}\frac{1}{(\mu\gamma)^n}g_L[\beta/\gamma^n] \tag{9}$$

and

$$f_L(\beta)=g_L(\beta)+\frac{1}{\mu\gamma}f_L\left(\frac{\beta}{\gamma}\right). \tag{10}$$

The general solution of Eq. (10) takes the same form as Eq. (7),

$$f_L(\beta)=\frac{1}{\beta^{1+m}}P_L\left(\frac{\ln\beta}{\ln\gamma}\right), \tag{11}$$

where $P_L(y)$ is an arbitrary periodic function of its argument y of period 1.

III. RECONSTRUCTION OF "WEIERSTRASS-TYPE FUNCTIONS" FROM POWER SERIES EXPANSIONS

Following [2,24], we use the Mellin transform to obtain a power-law series representation of the Weierstrass-type function (4). The Mellin transform is defined as

$$\hat{f}(s) \equiv \int_0^\infty x^{s-1} f(x) dx. \quad (12)$$

The Mellin transform (12) provides a reconstruction of the infinite sum of the Weierstrass-type function (4) as a sum of power-law contributions $A_n x^{-s_n}$ with ''universal'' complex exponents s_n determined only by properties of the hierarchical construction and not by the function $g(x)$, with amplitudes A_n controlled by the form of the regular part $g(x)$. These ''nonuniversal'' amplitudes in turn control the shape of the function $f(x)$, its differentiability or nondifferentiability as well as its self-affine (fractal) properties, as we shall describe in the sequel.

The Mellin transform of Eq. (4) reads

$$\hat{f}(s) = \frac{\mu\gamma^s}{\mu\gamma^s - 1} \hat{g}(s), \quad (13)$$

where $\hat{g}(s)$ is the Mellin transform of $g(x)$. The inverse Mellin transformation of $\hat{f}(s)$,

$$f(x) = \frac{1}{2\pi i} \int_{c-i\infty}^{c+i\infty} \hat{f}(s) x^{-s} ds, \quad (14)$$

allows us to reconstruct $f(x)$ as an expansion in singular as well as regular powers of x in order to unravel its self-similar properties. Indeed, the usefulness of the Mellin transform is that power-law behaviors spring out immediately from the poles of $\hat{f}(s)$, using Cauchy's theorem.

In inverting the Mellin transform, we have two types of poles. The poles of the Mellin transform $\hat{g}$ of the analytical function $g(x)$ occur in general at integer values and contribute only to the regular part $f_r(x)$ of $f(x)$, as expected since $g(x)$ is a regular contribution. The poles of the first term $[\mu\gamma^s/(\mu\gamma^s - 1)]$ in the right-hand side (r.h.s.) of Eq. (13) stem from the infinite sum over successive embeddings of scales and occur at $s = s_n$ where

$$s_n = -m + i\frac{2\pi}{\ln\gamma} n, \quad (15)$$

and m is given by Eq. (8). Their amplitude A_n is obtained by applying Cauchy's theorem and is given by the residues

$$\lim_{s \to s_n} \frac{s - s_n}{\mu\gamma^s - 1} \hat{g}(s) = \frac{\exp(-2\pi n i)}{\ln\gamma} \hat{g}(s) = \frac{\hat{g}(s)}{\ln\gamma}. \quad (16)$$

The resulting expression for $f(x)$ is

$$f(x) = f_s(x) + f_r(x), \quad (17)$$

where the singular part $f_s(x)$ is given by

$$f_s(x) = \sum_{n=0}^{\infty} A_n x^{-s_n} \quad (18)$$

and

$$A_n = \frac{\hat{g}(s_n)}{\ln\gamma}. \quad (19)$$

This approach is similar to the one developed in [25] for ''fractal strings'' η (for instance, the complementary of the triadic Cantor set is a special fractal string). Their fractal properties are fully characterized by the introduction of the ''geometric zeta function'' $\zeta_\eta(s)$, which can be shown to be nothing but the Mellin transform of the measure defined on the fractal string (see [25], p. 73). In particular, the poles of $\zeta_\eta(s)$ give the complex fractal dimensions of the fractal strings, similarly to the role played here by the complex exponents s_n defined by Eq. (15).

The regular part $f_r(x)$ of $f(x)$ defined in Eq. (17) is generated by the poles of $\hat{g}(s)$ if any, located at $s = -n$, $n = 0,1 \ldots$. The residues of these poles give the coefficients B_n of the expansion of the regular part as follows:

$$f_r(x) = \sum_{n=0}^{\infty} B_n x^n. \quad (20)$$

IV. CLASSIFICATION OF WEIERSTRASS-TYPE FUNCTIONS

A. Classification

The representation (18) offers a classification of Weierstrass-type functions as follows. We will work in the class of $g(x)$ [not covering of course all possible types of behavior of $A(n)$] where the coefficients A_n can be expressed as the product of an exponential decay by a power prefactor and a phase

$$A_n = \frac{1}{\ln\gamma} \frac{1}{n^p} e^{-\kappa n} e^{i\psi_n} \quad \text{for large} \quad n, \quad (21)$$

where p, $\kappa \geq 0$, and ψ_n are determined by the form of $g(x)$ and the values of μ and γ. This class is broad enough to include many physically interesting shapes of $g(x)$ as will be illustrated at length below.

1. Justification of the classification

The parameterization (21) can be seen to result from very general theorems on the Mellin transform [26,27]. Let us assume that the function $g(x)$ defined for $x > 0$ is continuous and satisfies the following conditions:

$$|g(x| \leq c_1 x^\alpha, \quad 0 < x \leq 1; \quad |g(x| \leq c_2\, x^\beta, \quad 1 \leq x < \infty, \quad (22)$$

where $\alpha > \beta$. Then, its Mellin transform is a regular (differentiable) function inside the strip $-\alpha < \mathrm{Re}(s) < -\beta$. One should also bear in mind that $\mathrm{Re}(s) < 0$ because of the constraints imposed by the very formulation of the problem. All functions that we shall consider below as examples belong to the class of continuous functions satisfying slightly more restricted conditions [26] such as Eq. (22) with $\alpha > 0$ and $\beta = 0$. As a consequence, their Mellin transform is regular for $-\alpha < \mathrm{Re}(s) < 0$. For instance, $g(x) = \cos(x) - 1$ corresponds to $\alpha=1$ and $\beta=0$. The same conditions apply to $\ln(1+x)$ and $\exp(-x)-1$. For the stretched exponential function $\exp(-x^h)-1$ with $h>0$, we have $\alpha=h$ and again $\beta=0$.

We are interested in $\widehat{g(s_n)}=\hat{g}(-m+in\omega)$, particularly as n goes to infinity. The general condition that is usually imposed on this quantity in order to ensure the existence of its inverse Mellin transform is [27]

$$\hat{g}(-m+in\omega)\to 0 \quad \text{as} \quad n\to+\infty. \tag{23}$$

Again, A_n must be designed in such a way that it satisfies this condition automatically.

Let us consider some simple but vivid examples, intended to illustrate how a power-law and exponential decay of A_n as a function of n emerges from simple functions satisfying the conditions stated above. We also note that, when $g(t)$ possesses discontinuities of the first kind, it still yields the dependence Eq. (21) of A_n as a function of n. Maybe the simplest function leading to A_n with a power-law decay is

$$g(x)=0, \quad 0<x<1 \quad \text{and} \quad g(x)=-1, \quad 1<x<\infty, \tag{24}$$

which leads to $\widehat{g(s)}=1/s$, which is regular within the strip $\infty<\mathrm{Re}(s)<0$. The corresponding A_n decays in amplitude as n^{-1} for large n. Different strip geometries lead to the same power-law decay of A_n, for instance

$$g(x)=x^a, \quad 0<x<1 \quad \text{and} \quad g(x)=0, \quad 1<x<\infty, \tag{25}$$

with Mellin transform $\widehat{g(s)}=(s+a)^{-1}$ with $-a<\mathrm{Re}(s)<0$. Let us also consider

$$g(x)=0, \quad 0<x<1 \quad \text{and} \quad g(x)=-x^a, \quad 1<x<\infty, \tag{26}$$

which leads to a similar Mellin transform $\widehat{g(s)}=(s+a)^{-1}$ but a different strip geometry $\mathrm{Re}(s)<-a$. The slightly more complicated example of a continuous function composed of power laws

$$g(x)=(b-a)^{-1}x^a, \quad 0<x<1$$

and

$$g(x)=(b-a)^{-1}x^b, \quad 1<x<b, \tag{27}$$

leads to $\widehat{g(s)}=(s+a)^{-1}(s+b)^{-1}$ with $-a<\mathrm{Re}(s)<-b$ and the amplitude of A_n decaying as n^{-2}. The analysis of these examples and of their Mellin transforms at $s=s_n$ demonstrate that particulars of the strip geometry in the variable s are not important when one is concerned with the large n asymptotic behavior of $\hat{g}(s_n)$. The asymptotic power decay of A_n as a function of n can be dominated by an exponential decay, as we shall see in more details below. For instance, the continuous function formed by compounded power laws $g(x)=(1/\pi)x(1+x)^{-1}$ leads to

$$\widehat{g(s)}=-\csc(\pi s), \quad -1<\mathrm{Re}(s)<0,$$

yielding A_n decaying as $\exp(-n)$ as $n\to+\infty$.

Violations of the parameterization (21) regarding A_n occur when the conditions of the theorem [26] are changed, e.g., when the argument x is replaced by, say, $\ln(1/x)$ or when singularities are introduced into the function $g(x)$. This can be seen from Eq. (19) that shows that A_n is proportional to the Mellin transform of $g(t)$ expressed at $s=s_m=-m+in\omega$ where

$$\omega=\frac{2\pi}{\ln\gamma}. \tag{28}$$

Posing $u=\ln x$, the Mellin transform becomes a Fourier transform

$$A_n=\frac{1}{\ln\gamma}\int_{-\infty}^{+\infty}du\, G(u)e^{i\omega n u}, \tag{29}$$

where

$$G(u)\equiv e^{u(1-m)}g(e^u). \tag{30}$$

It is clear that, by a suitable choice of $g(x)$, any dependence of A_n can be obtained. For instance, for

$$G(u)=u^{-3/2}e^{-a/u}, \tag{31}$$

we obtain $A_n\sim e^{-\sqrt{2an}}\cos[\sqrt{2an}]$, which exhibits an oscillatory stretched-exponential decay intermediate between the exponential ($\kappa>0$) and pure power-law decay ($\kappa=0$) of Eq. (21). However, the choice Eq. (31) corresponds to a rather special choice for

$$g(x)=\frac{(\ln x)^{-3/2}e^{-a/\ln x}}{x^{1-m}}. \tag{32}$$

In this case, $g(x)\to+\infty$ for $x\to 0$, and this case is outside the domain of validity (22) of the theorem [26,27]. Consider also the following example

$$g(x)=\pi^{-1/2}\exp\left(-\frac{\ln(1/x)^2}{4}\right), \tag{33}$$

leading to $\widehat{g(s)}=\exp(s^2)$, valid for arbitrary s, which leads to A_n with amplitude decaying as $\exp(-n^2)$ as $n\to\infty$. This example is also characterized by a pathological behavior for $x\to+\infty$ of $g(x)$ that diverges faster than any power law. Another pathological example is

$$g(x)=1/2\pi^{-1/2}\cos[(1/4)\ln(1/x)^2-\pi/4], \tag{34}$$

leading to $\widehat{g(s)}=\cos s^2$, valid for arbitrary s, which yields A_n with an amplitude growing as $\exp(n)$ as $n\to+\infty$. This violates the condition on the Mellin transform given in [27].

The existence of discontinuities of $g(x)$, as one might expect from the theorem [26,27], also violates the parameterization (21) of A_n. Consider $g(x)=-(1/\pi)x^{1/2}(1-x)^{-1}$ with an integrable singularity, which gives $\widehat{g(s)}=\tan(\pi s)$, $-1/2<\mathrm{Re}(s)<0$, and A_n with an amplitude bounded from below by a constant as $n\to+\infty$. This absence of decay allows us to reject this type of function, since a decay of A_n is required by [27]. In constrast, a logarithmic singularity, as for instance in $g(x)=(1\pi)\ln|(1+x)/(1-t)|$, is allowed. In this case, this gives $\widehat{g(s)}=s^{-1}\tanh(\pi s), -1<\mathrm{Re}(s)<0$, and the amplitude of $\widehat{g(s_n)}$ exhibits periodic modulations as $n\to+\infty$ as $n^{-1}[\sinh^2(\frac{1}{2}\pi m)+\cos^2(\frac{1}{2}\pi\omega n)]^{-1}[\sin(\pi\omega n)+i\sinh(\pi m)]$. Another example with the logarithmic function (93) discussed below gives a power-law decay with a logarithmic correction as shown by Eq. (95) due to the presence of the singularity.

In conclusion, as long as the conditions of theorem [26] on Mellin transforms hold, the dependence of A_n as $n\to+\infty$ given by Eq. (21) will hold as well. Violations of the theorem due to a change of variable or to the presence of simple poles lead either to a faster decay or to a nondecaying A_n. Allowing for logarithmic singularities within $g(x)$ brings in logarithmic or oscillatory corrections to A_n as a function of n.

2. Beyond the linear approximation of the renormalization group map

The asymptotic expansion (21) uses the linear approximation $R^{(n)}(x)=\gamma^n x$ that allows us to transform the general solution (3) into the Weierstrass-type function (4). As we said, Eq. (4) is only applicable sufficiently "close" to the critical point $x=0$, such that the higher-order terms in the expansion $R(x)=\gamma x$ can be neglected. The linear approximation of $R^{(n)}(x)=\gamma^n x$ is bound, however, to become incorrect as n becomes very large, i.e., in the region determining the singular behavior. As discussed in [2,24], the crucial property missed by the linear approximation is that $f(x)$ is analytic only in a sector $|\arg x|<\theta$ while we treated it as analytic in the cut plane $|\arg x|<\pi$. This implies that the exponential contribution $e^{-\kappa n}$ of the true asymptotic decay of the amplitudes of successive log-periodic harmonics is slower than found from the linear approximation, and goes as $e^{-\kappa\theta n}$. The angle θ depends specifically on the flow map $R(x)$ of the discrete renormalization group [2] and is generally of order 1. Our classification in two sets $\kappa=0$ and $\kappa\neq 0$ is not modified by this subtlety. Here, we shall consider only the Weierstrass-type functions (4) and will revisit the impact of nonlinear terms of the renormalization group map in a future communication.

3. $\kappa>0$: C^∞ differentiability

The general solution (7) remains true for any choice of the regular part $g(x)$ with the exponent m given by Eq. (8). This implies that there will always be an order of differentiation sufficiently large such that it becomes infinite at $x=0$ [12]. This is the crux of the argument on the existence of the singularity at $x=0$. Here, we investigate the differentiability of $f(x)$ for nonzero values of x, i.e., away from the unstable critical point $x\to 0$. Expression (18) with Eq. (15) provides a direct way for understanding the origin of the singular behavior at $x\to 0$, as x^m is in factor of an infinite sum of oscillatory terms with log-periodic oscillations condensing geometrically as $x\to 0$.

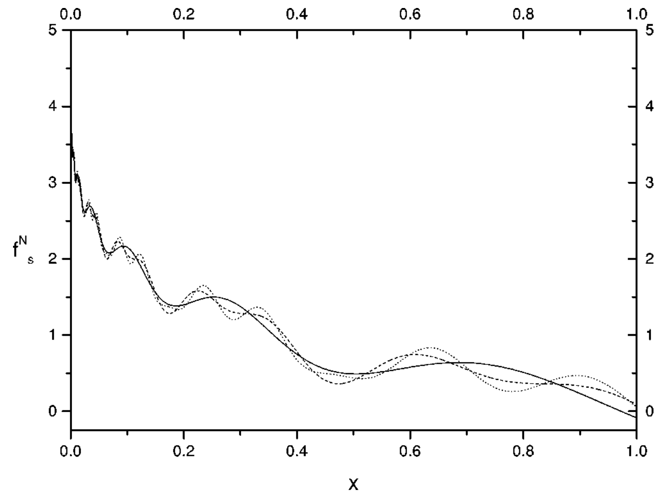

FIG. 1. Power-law expansion part f_s given by Eq. (18) for the Weierstrass function (5), with $N=1$ (solid), $N=2$ (dash), $N=3$ (dot) oscillatory terms, respectively. Here, $m=0.25, \omega=6.3$ corresponding to $\gamma=2.7$ and $\mu=1.28$. As the number of complex exponents increases, the number of the oscillations increase.

When $\kappa>0$, the modulus of A_n decay exponentially fast to zero. Hence, $f(x)$ is differentiable at all orders. This can be seen from the fact that

$$\frac{d^{\ell}f_s(x)}{dx^{\ell}}=\sum_{n=0}^{\infty}(-s_n)(-s_n-1)\cdots(-s_n-\ell+1)A_n x^{-s_n-\ell} \tag{35}$$

is absolutely convergent for any order ℓ of differentiation. Taking into account that $|x^{-s_n-\ell}|=x^{m-\ell}$ is independent of n and can be factorized, the nth term in the sum has an amplitude bounded by a constant times $n^{\ell}\exp[-qn]$ since $(-s_n)\times(-s_n-1)\cdots(-s_n-\ell+1)$ is bounded from above by a constant times n^{ℓ}. The sum is thus controlled by the exponentially fast decaying coefficients A_n and converges to well-defined values for any ℓ. As a consequence of the exponential decay of the coefficients A_n, the log-periodic oscillations are extremely small.

Another obvious way to ensure differentiability even when $\kappa=0$ (see the following section) is to truncate the number n of powers x^{-s_n} in the sum (18) to a finite value

$$f_s^{(N)}(x)=\sum_{n=0}^{N}A_n x^{-s_n}. \tag{36}$$

An example with $N=1,2,3$ is shown in Fig. 1 for the Weierstrass function ($\alpha=\pi/2$ and $p=m+\frac{1}{2}$). For $N=1$, the real part $f_s^{(1)}(x)$ is given by

$$f_s^{(1)}(x)=a_0\left[1+\frac{A_{n=0}}{a_0}x^m+\frac{|A_{n=1}|}{a_0}x^m\cos[\omega\ln(x)+\varphi)\right],$$

$$a_0=\frac{\mu}{\mu-1}, \tag{37}$$

where ω is given by Eq. (28) and

$$\varphi = \arctan\left(\frac{\text{Im}(A_{n=1})}{\text{Re}(A_{n=1})}\right) + k\pi, \quad k=0,\pm 1,\ldots. \tag{38}$$

This expression (37) is based on the singular part (18) of the Mellin decomposition of the discrete-scale invariance (DSI) Eq. (4). It applies not only to the Weierstrass function but also to any function of the form (4). Keeping only the first two terms recovers exactly the log-periodic formula introduced in the study of precursors of material failure [5,28,29], earthquakes precursors [6,30,31], and of precursors of financial crashes [7,32].

4. Critical behavior and nondifferentiability

Expression (18) with Eqs. (15) and (21) shows that $f_s(x)$ has the same differentiability properties as

$$\sum_{n=1}^{+\infty} \frac{1}{n^p} e^{i\psi_n} x^{m-i2\pi n/\ln\gamma}. \tag{39}$$

Changing variable $x \to y = \ln x/\ln\gamma$, this reads

$$e^{y\ln\mu} \sum_{n=1}^{+\infty} \frac{1}{n^p} \exp[i(-2\pi n y + \psi_n)]. \tag{40}$$

With respect to the differentiability property, it is sufficient to study the real part of the infinite sum that reads

$$K_{p,\{\psi_n\}}(y) = \sum_{n=1}^{+\infty} \frac{\cos[2\pi n y + \psi_n]}{n^p}. \tag{41}$$

This expression allows us to recover some important results in the case where the phases ψ_n are sufficiently random so that the numerators $\cos[2\pi ny + \psi_n]$ take random uncorrelated signs with zero mean. Then, the sum $K_{p,\{\psi_n\}}(y)$ truncated at $n=T$ has the same convergence properties for $T\to\infty$ as

$$X(T) = \int_1^T \frac{dW_t}{t^p}, \tag{42}$$

where dW_t is the increment of the continuous white noise Brownian motion of zero mean and correlation function $\langle dW_t dW_{t'}\rangle = \delta(t-t)dt$ where δ is the Dirac function. We get $\langle X(T)\rangle = 0$ and its variance is

$$\langle [X(T)]^2\rangle = \int_1^T\int_1^T \langle dW_t dW_{t'}\rangle t^{-p} t'^{-p} = \int_1^T \frac{dt}{t^{2p}}, \tag{43}$$

which is finite for $T\to+\infty$ if $p>1/2$. This entails the convergence for $p>1/2$ of the infinite series (41) for most phases ψ_n that are sufficiently ergodic and mixing. We thus expect that $K_{p,\{\psi_n\}}(y)$ and as a consequence $f_s(x)$ are continuous functions for $p>1/2$. We can proceed similarly for studying their ℓ's derivative. With respect to the convergence property, taking the ℓ's derivative has the effect of changing p into $p-\ell$ in Eq. (42). We thus expect $K_{p,\{\psi_n\}}(y)$ and as a consequence $f_s(x)$ to be differentiable of order ℓ for $p>\ell+1/2$.

We conjecture the following conditions for nondifferentiability from the singular power-law expansion of Weierstrass-type functions. Provided that (1) $\kappa=0$ and (2) the phases ψ_n are ergodic and, using a generalization of Hardy's condition $ab>1$ for the Weierstrass function, the smallest order $\ell_{\min}$ of differentiation of $f_s(x)$ [defined by Eq. (18) with exponents s_n given by Eq. (15) with Eq. (8)] that does not exist is such that

$$\frac{1}{2} < p - \ell_{\min} < \frac{3}{2}, \tag{44}$$

i.e.,

$$\ell_{\min} = \text{Int}\left[p - \frac{3}{2}\right], \tag{45}$$

is the integer part of $p-\frac{3}{2}$. In particular, with ergodic phases ψ_n of zero mean, the function $f_s(x)$ is nondifferentiable for $p<3/2$.

It follows from Lebesgue's theorem on continuous functions of bounded variations that a nondifferentiable function is not a function of bounded variation. Therefore, a nondifferentiable function is everywhere oscillating and the length of arc between any two points on the curve is infinite [21]. This explains the observation below that the regular part $g(x)$ must contain oscillations or must exhibit a compact support (so that it has a discrete Fourier series) in order for $f(x)$ to be nondifferentiable or for some of its derivatives to be nondifferentiable. Actually, Weierstrass-type functions (4) are believed to have the same Hausdorff dimension $2-m$ as the Weierstrass function (5) for arbitrary regular part $g(x)$, as long as it is a bounded almost periodic Lipschitz function of order $\beta>m$ [34]. The examples organized below in two classes illustrate and make precise this condition on $g(x)$. We indeed find that nondifferentiability occurs at a finite order of differentiation only for functions $g(x)$ that are periodic or with compact support.

It appears, however, that there is not yet a general understanding of whether there exists a necessary and sufficient condition for the differentiability of a function on an interval. It is well known that continuity is necessary for differentiability but is not sufficient as shown by the Weierstrass function and other examples above. The restriction of bounded variations has also proved insufficient: although a continuous function must possess a differential coefficient almost everywhere, yet there are examples of such functions that do not possess differential coefficients at unenumerable sets of points that are everywhere dense [21].

B. General condition for $\kappa=0$

Let us consider a regular function $g(x)$ that is either periodic with period X or with compact support over the interval $[0,X]$ and zero outside. It can then be expanded as a Fourier series

$$g(x)=\frac{a_0}{2}+\sum_{k=1}^{+\infty}[a_k\cos(2\pi kx/X)+b_k\sin(2\pi kx/X)], \tag{46}$$

where $a_0,a_1,b_1,\ldots,a_k,b_k,\ldots$ are arbitrary real numbers.

The behavior of the coefficients A_n is controlled by the Mellin transform $\hat{g}(s_n)$ of $g(x)$ as shown by Eq. (19). For $g(x)$ periodic with zero mean, $a_0=0$ and

$$\hat{g}(s_n)=\left(\frac{X}{2\pi}\right)^{s_n}\left[\widehat{\cos}(s_n)\sum_{k=1}^{+\infty}\frac{a_k}{k^{s_n}}+\widehat{\sin}(s_n)\sum_{k=1}^{+\infty}\frac{b_k}{k^{s_n}}\right], \tag{47}$$

where $\widehat{\cos}(s)$ and $\widehat{\sin}(s)$ are the Mellin transform of $\cos x$ and $\sin x$. Now, a general theorem on the Fourier series of periodic functions tells us that, if $g(x)$ has continuous derivatives up to order r included and if the derivative of order k obeys the Dirichlet conditions, then the coefficients a_k and b_k decay for large k as $1/k^{r+1}$, i.e., there is finite $M'>M>0$ such that $M'/k^{r+1}>|a_k|>M/k^{r+1}$ and $M'/k^{r+1}>|b_k|>M/k^{r+1}$. If $g(x)$ is discontinuous at a discrete set of points, this corresponds to taking $r=0$ in the previous formula. The Dirichlet conditions are: (i) $g(x)$ is continuous or possess only a finite number of discontinuities; (ii) each point of discontinuity x_d is a discontinuity of the first kind, i.e., it is such that the limits to the left $g(x\to x_d^-)$ and to the right $g(x\to x_d^+)$ are finite; (iii) the interval $[0,X]$ can be divided into a finite set of subintervals on each of which $g(x)$ is monotonic.

We can thus write

$$2M\left(\frac{X}{2\pi}\right)^{s_n}\widehat{\sin}(s_n)\sum_{k=1}^{+\infty}\frac{k^{-in\omega}}{k^{r+1-m}} <\hat{g}(s_n)<2M'\left(\frac{X}{2\pi}\right)^{s_n}\widehat{\sin}(s_n)\sum_{k=1}^{+\infty}\frac{k^{-in\omega}}{k^{r+1-m}}. \tag{48}$$

The sum

$$\sum_{k=1}^{+\infty}k^{-(r+1-m+in\omega)}, \tag{49}$$

is nothing else but the celebrated zeta function $\zeta(y)$ of Riemann [35,36], with the correspondence $y=\sigma+it$, $\sigma=r+1-m$, $t=n\omega$. It is known [35,36] that $|\zeta(\sigma+it)|\leqslant C_\sigma(|t|+1)^{1/2-\sigma}$ for $\sigma<0$, where C_σ decreases such as $(2\pi e)^{\sigma-1/2}$ for $\sigma\to-\infty$, and it does not satisfy a better estimate in this half plane. For $0\leqslant\sigma\leqslant 1$ corresponding to $0\leqslant m\leqslant 1$ and $p=0$, $\zeta(\sigma+it)|\leqslant Kt^{(1-\sigma)/2}\ln(t)$ uniformly for some constant K. However, we need the behavior of $\zeta(\sigma+it)$ for $\sigma=r+1-m>0$. It is obtained by using the relation $\zeta(s)=2^s\pi^{s-1}\sin(\pi s/2)\Gamma(1-s)\zeta(1-s)$, which can be separated into two parts that can be evaluated. Namely, $\sin([\pi/2s]\Gamma(1-s)$, recast in the variable $z=1-s$, takes the familiar form $\cos([\pi/2]z)\Gamma(z)$, which behaves for large n as $n^{-r+m-1/2}$. The other term $\zeta(1-s)=\zeta(z)$ can be evaluated using the expression presented above for the ζ function of an argument with negative real part (in our case for negative $1-\sigma$ and large n), $\zeta(z)\leqslant C(|n|+1)^{1/2-(1-\sigma)}=C(|n|+1)^{1/2+r-m}$. Therefore, the product of these two terms is of the order of C and the whole sum decay is slower than exponential.

This shows that the sum (49) is of order $O(1/n^{r+(1/2)-m})$ and thus $\hat{g}(s_n)$ is asymptotically a negative power of n for large n. This demonstrates that any periodic continuous function $g(x)$ leads to a power-law decay for A_n as a function of n.

The same approach can be used for $g(x)$ not periodic but defined on a compact support $[0,X]$. The discrete Fourier series expansion (46) still holds for $x\in[0,X]$ while $g(x)=0$ for x outside. A similar expression to Eq. (47) then holds in which $a_0\neq 0$ in general and in which the Mellin transforms $\widehat{\cos}(s)$ and $\widehat{\sin}(s)$ are defined over the interval $[0,X]$.

C. Bifurcation from wild to smooth Weierstrass-type functions: An example using damped oscillators for the regular part of the renormalization group equation

As a first example, let us consider the regular part $g(x)$ of the renormalization group equation defined as

$$g(x)=e^{-\cos(\alpha)x}\cos[x\sin(\alpha)],\quad \text{with}\quad \alpha\in\left[0,\frac{\pi}{2}\right]. \tag{50}$$

The parameter α quantifies the relative strength of the oscillatory structure of $g(x)$ versus its "damping." For $\alpha=\pi/2$, Eq. (4) with Eq. (50) recovers the initial function (5) introduced by Weierstrass with $b=1/\mu$, $a=\gamma$, and $\cos(\pi x)$ replaced by $\cos(x)$; for $\alpha=0$, $g(x)=\exp[-x]$ has no oscillation anymore and corresponds to a pure exponential relaxation considered in [33].

Plugging Eq. (50) in Eq. (4) gives

$$f(x)=\sum_{n=0}^{\infty}\frac{1}{\gamma^{(2-D)n}}\exp[-\cos(\alpha)\gamma^n x]\cos[\gamma^n x\sin(\alpha)], \tag{51}$$

where

$$D=2-m=2-\frac{\ln\mu}{\ln\gamma}. \tag{52}$$

The exponent D turns out to be equal to the fractal dimension of the graph of the Weierstrass function obtained for $\alpha=\pi/2$. Recall that the fractal dimension quantifies the self-similarity properties of scale-invariant geometrical objects. Note that $1<D<2$ as $1<\mu<\gamma$, which is the condition of nondifferentiability found by Hardy [20] for the Weierstrass function. The graph of the Weierstrass function is thus more than a line but less than a plane. For $\alpha<\pi/2$, $f(x)$ is smooth, nonfractal $(D=1)$, and its graph has the complexity of the line. Actually, there are several fractal dimensions. It is known that the box counting (capacity, entropic, fractal, Minkowski) dimension and the packing dimensions of the Weierstrass function are all equal to D [37] given by Eq. (52)

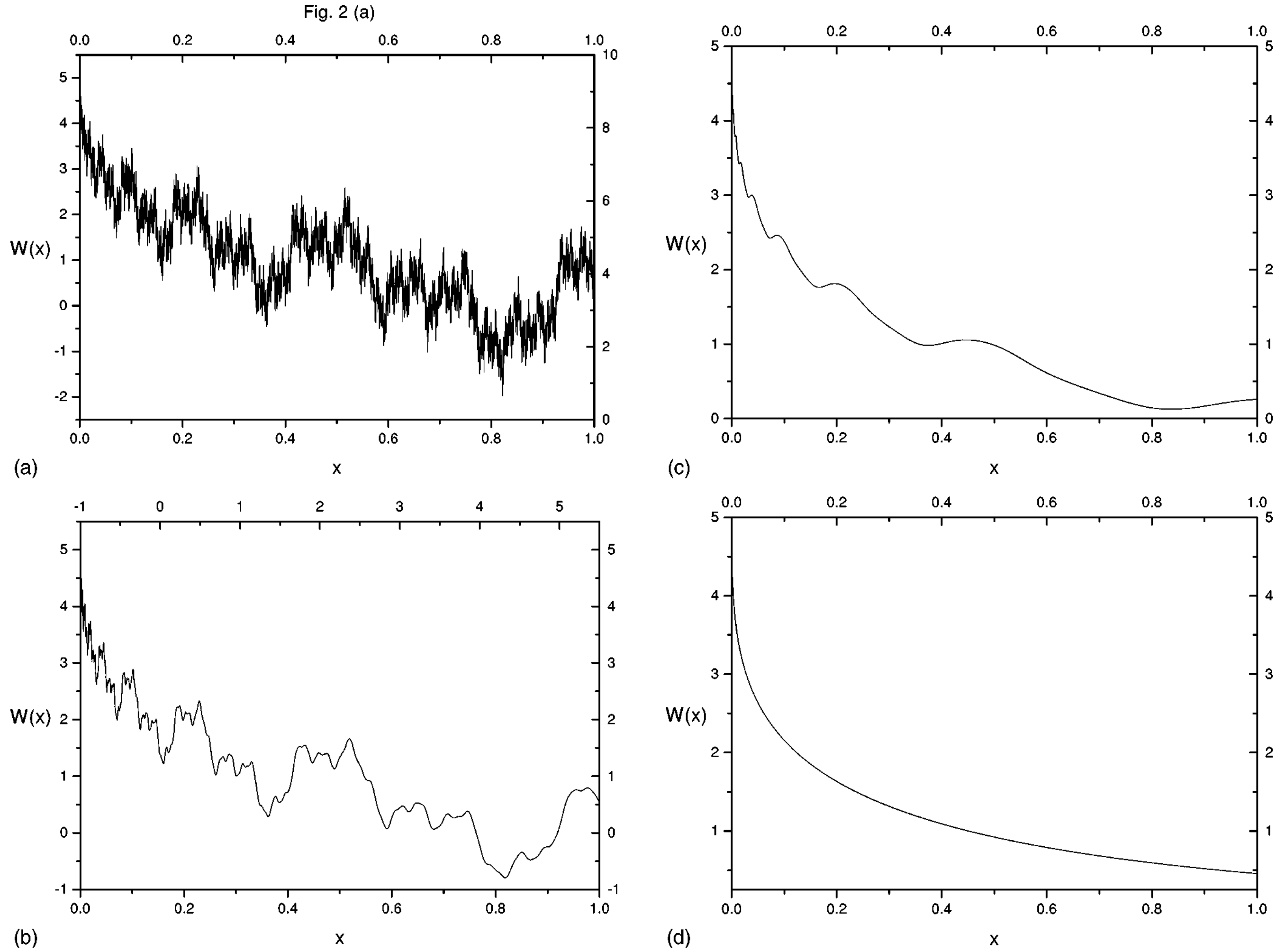

FIG. 2. Quasi-Weierstrass function for (a) $\alpha=\pi/2$, (b) $\alpha=0.993\pi/2=1.56$, (c) $\alpha=0.9\pi/2=1.414$, and (d) $\alpha=0$, for $m=0.25,\omega=7.7$, using $N=32$ terms to estimate the sums (51). Increasing N does not change the results.

for $\alpha=\pi/2$. It is conjectured but not proved that the Hausdorff fractal dimension of the graph of the Weierstrass function obtained for $\alpha=\pi/2$ is also equal to D given by Eq. (52). It is known that the Hausdorff dimension of the graph of $f(x)$ does not exceed D but there is no satisfactory condition to estimate its lower bound [34].

Figure 2 shows the function (51) for $\alpha=\pi/2=1.5708$ (pure Weierstrass function: panel a), $\alpha=0.993\pi/2=1.56$ (panel b), $\alpha=0.9\pi/2=1.414$ (panel c), and $\alpha=0$ (panel d).

The Mellin transform of $g(x)$ defined by Eq. (50) for $-1<\mathrm{Re}[s]=-m<0$ [which is the interval of interest, as seen from Eq. (15)] is [38]

$$\hat{g}(s)=\Gamma(s)\cos(\alpha s)-\frac{1}{s}, \tag{53}$$

where $\Gamma(s)$ is the gamma function reducing to $\Gamma(s)=(s-1)!$ for integer arguments s. The additional term $-1/s$ disappears for $0<\mathrm{Re}[s]$. For values of the exponent m larger than 1, i.e., $\mathrm{Re}[s]<-1$, additional correction terms should be added to Eq. (53) [38]. These additional terms only contribute to the power-law dependence of the amplitudes A_n and not to the exponential. This problem is absent when the cosine in the definition of $g(x)$ is replaced by the sine function.

As we shall discuss below, the modification of $g(x)$ into the modified function

$$g_M(x)=e^{-\cos(\alpha)x}\cos[x\sin(\alpha)]-1 \tag{54}$$

gives $\hat{g}(s)=\Gamma(s)\cos(\alpha s)$ without the correction $-1/s$ for $-1<\mathrm{Re}[s]=-m<0$ and leads to the so-called Mandelbrot-Weierstrass function. Similar "counterterm" should be introduced for stretched exponential and in similar cases. They do not bring any extra contributions to the Mellin transform.

The regular part $f_r(x)$ defined by Eq. (20) of $f(x)$ defined in Eq. (17) corresponding to $g(x)$ defined by Eq. (50) is generated by the poles of $\Gamma(s)$, located at $s=-n$, $n=0,1\ldots$, since $\Gamma(s)$ is analytic on the whole complex plane excluding these simple poles [39]. Using the expression $\mathrm{Re}\, s_{s=-n}\Gamma(s)=(-1)^n/n!$, we obtain its explicit form (20) with

$$B(n)=\frac{(-1)^n}{n!}\,\frac{\mu}{\mu-\gamma^n}\cos(\alpha n). \tag{55}$$

Note the particularly simple expression of the first term $B_0 = \mu/(\mu-1)$. For $|x|\ll 1$, this constant term provides the only non-negligible contribution of the regular part $f_r(x)$ to $f(x)$, whose behavior is completely controlled by the sum $f_s(x)$ of singular power laws.

The amplitudes A_n defined by Eq. (19) corresponding to $g(x)$ defined by Eq. (50) are

$$A_n(\alpha)=\frac{\Gamma(s_n)\cos(\alpha s_n)}{\ln\gamma}. \tag{56}$$

The singular part $f_s(x)$, which is defined by Eq. (18) where the exponents s_n are given by Eq. (15), satisfies the exact scale-invariance equation (1).

The asymptotic behavior of the amplitudes A_n given by Eq. (56) is

$$A_n(\alpha)\sim\frac{e^{\alpha m}}{n^{m+1/2}}\exp\left[-\omega n\left(\frac{\pi}{2}-\alpha\right)\right]e^{i\omega n\ln(\omega n)}, \quad n\to\infty, \tag{57}$$

with $m=(\ln\mu)/(\ln\gamma)$. The angular log frequency ω is defined by Eq. (28). In order to obtain Eq. (57), we have used the asymptotic dependence of the Γ-function asymptote for complex z [39]

$$\Gamma(z)\simeq e^{(z-1/2)\ln z-z}, \quad |z|\gg 1. \tag{58}$$

Expression (57) is of the form (21) with $p=m+\frac{1}{2}$, $\kappa=\omega([\pi/2]-\alpha)$, and $\psi_n=\omega n\ln(\omega n)$.

For $\alpha=0$,

$$A_n(0)\sim\frac{1}{n^{m+(1/2)}}e^{-(\pi/2)\omega n}e^{i\omega n\ln(\omega n)}, \quad n\to\infty. \tag{59}$$

As we have shown above, the fast exponential decay of $A_n(0)$ ensures the differentiability of $f(x)$ at all orders. Actually, the fast decay of $A_n(0)$ washes out any observable oscillatory structure from the function as seen in Fig. 2(d). However, there are very tiny log-periodic oscillations of amplitude less than 5×10^{-7} (see Table I) that are, however, unobservable at the scale of the plot of Fig. 2(d).

For $\alpha=\pi/2$ (Weierstrass function), the exponential part disappears and

$$A_n(\pi/2)\sim\frac{1}{n^{m+1/2}}e^{i\omega n\ln(\omega n)}, \quad n\to\infty. \tag{60}$$

This situation corresponds to the case $p=m+\frac{1}{2}$, $\kappa=0$, and $\psi_n=\omega n\ln(\omega n)$ in expression (21) of the classification of Sec. IV A. The cancellation of the exponential term in A_n is due to the very peculiar compensation of the exponential decay of $\Gamma(s_n)$ by the exponential growth of $\cos(\alpha s_n)$ in Eq. (53), which occurs only for $\alpha=\pi/2$.

The original Weierstrass function (5) is thus seen as a very special "critical" or bifurcation point of the class of Weierstrass-type functions (4) with Eq. (50). The analogy goes further as the expression (21) for the amplitudes A_n has the same structure as the correlation function of a system of spins where the order n in the sum (18) plays the role of the distance r between two spins. In this analogy, the "correlation length" is proportional to $1/\kappa\sim([\pi/2]-\alpha)^{-1}$ and diverges at the critical point $\alpha=\pi/2$.

D. Role of the phase: Localization and delocalization of singularities

The phases ψ_n defined in Eq. (21) play an essential role in the construction of the self-affine nondifferentiable structure of the Weierstrass-type functions. To stress this fact, let us consider several cases using different phases ψ_n with the same absolute values $|A_n|$ of the amplitudes. This study parallels in a sense that of Berry and Lewis [41] and of Hunt [42] but is distinct from it in an essential way as the phases considered here decorate the amplitudes A_n in Eq. (18) of the power series expansion, rather than the phases of the cosine in Eq. (5). Actually, Berry and Lewis study a slight modification of the Weierstrass function (5) defined as

$$f_{WM}=\sum_{n=0}^{\infty} b^n(1-\cos[a^n\pi x]), \tag{61}$$

proposed by Mandelbrot [43], which has the property of directly satisfying the "self-affine" property (1) with $\mu=1/b$ and $\gamma=1$. As discussed above, the choice Eq. (54) for $g(x)$, which gives Eq. (61) up to a sign, has the advantage of getting rid of the $-1/s$ correction in its Mellin transform (53) that makes thus more apparent and direct its self-similar properties.

Hunt [42] is able to show that, by replacing the argument $a^n\pi x$ of the cosine by $a^n\pi x+\theta_n$, where θ_n, are uncorrelated random phases, the Hausdorff dimension of the phase-randomized Weierstrass function is $D=2-m$.

1. Localization of singularities

Let us first study the case where ψ_n is put equal to 0, i.e., we construct a phase-locked Weierstrass function as

$$\overline{f_s(x)}=\sum_{n=0}^{\infty}|A_n(\pi/2)|x^{-s_n}, \tag{62}$$

i.e., by constructing the singular part as the sum over power laws with amplitudes equal to the modulus of the amplitudes (56) obtained for the Weierstrass function with $\alpha=\pi/2$, i.e., $|A_n(\pi/2)|=|\{\Gamma(s_n)\cos[(\pi/2)s_n]\}/\ln\gamma|$, but without the phase. As a consequence, Eq. (60) is changed to

$$|A_n(\pi/2)|=C\frac{1}{n^{m+(1/2)}}, \quad \text{for} \quad n\to\infty, \tag{63}$$

where C is a constant.

Figure 3 shows the function $\overline{f_s(x)}$ defined by Eq. (62) for $m=0.2$ (panel a) and $m=0.65$ (panel b). Rather than the familiar nondifferentiable self-affine corrugated structure of the Weierstrass function, $\overline{f_s(x)}$ seems to be differentiable everywhere except for a discrete infinity of spikes at positions x_u, where u is an integer running from $-\infty$ to $+\infty$, orga-

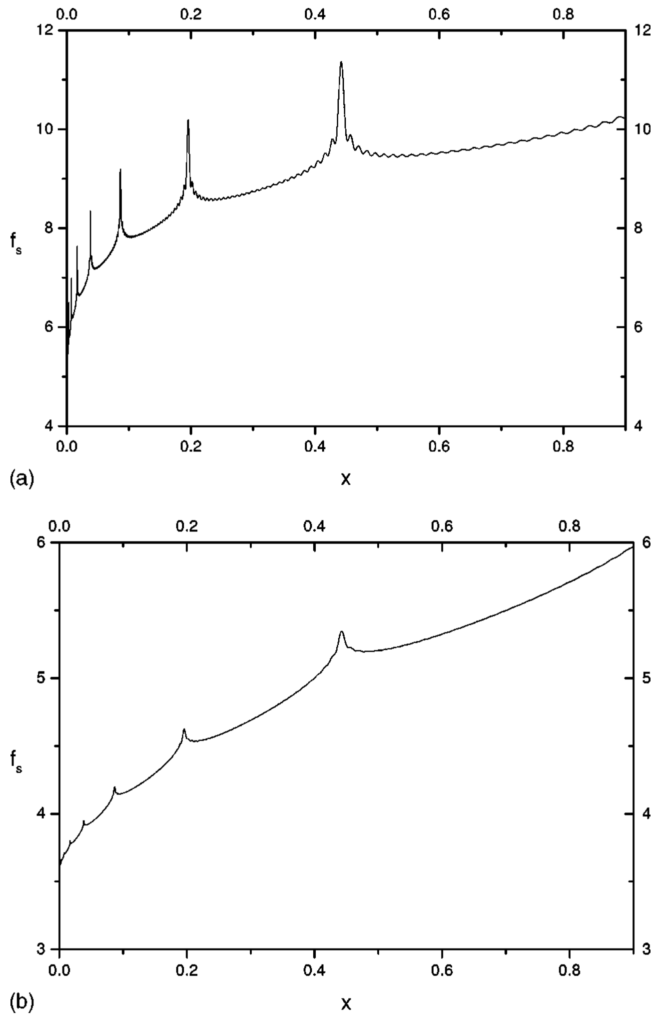

FIG. 3. Panels *a* and *b* show $f_s(x)$ defined by Eq. (62) with zero phase $\psi_n=0$ for $m=0.2$ and $m=0.65$, respectively, with the same $\omega=7.7$, constructed by truncating the sum at the $N=29$ term. The tiny regular oscillations result from the truncation to a finite N and slowly vanish when $N\to\infty$. They are thus spurious finite-size effects.

nized according to a geometric log-periodic structure. This discrete set of spikes decorates the leading singular behavior $f(x)\sim x^m$ for $x\to 0$ of the general solution (7). Note that, in this case, the periodic function $P([\ln x]/[\ln \gamma])$ of the general solution (7) is formed by the set of spikes geometrically converging to the origin.

The spikes seem to diverge for $m=0.2$ while they converge to a finite value for $m=0.65$, as far as the numerical construction suggests. Appendix A examines some differentiability properties of Eq. (62). Appendix B shows that the functional shapes of the spikes for $x\to x_u=1/\gamma^u$ with u integer are given by

$$G_s(x)\sim \frac{1}{|x-x_u|^{(1/2)-m}}. \tag{64}$$

Thus, for $0<m<1/2$ (panel *a* of Fig. 3), the spikes correspond to a divergence of $G_s(x)$ as $x\to x_u$. For $1/2<m<3/2$, $G_s(x)$ goes to a finite value as $x\to x_u$ but with an infinite slope (since $0<m-\frac{1}{2}<1$) according to $G_s(x)\sim \text{constant}-|x-x_u|^{m-(1/2)}$.

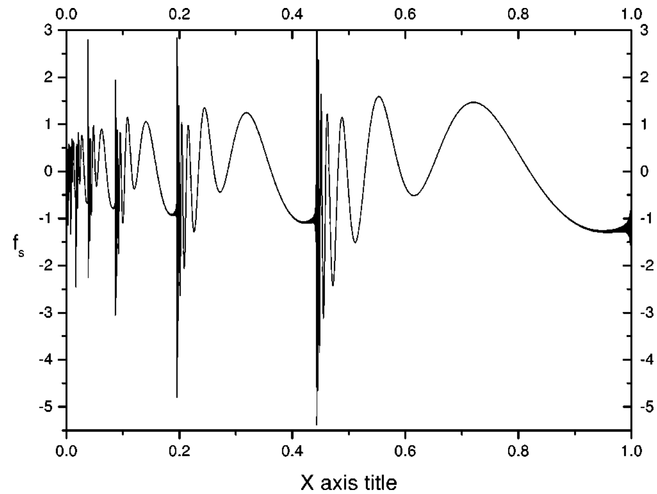

FIG. 4. Graph of $f_s(x)$ defined by Eq. (65) with $\psi_n=\omega\ln(\omega n)$, $m=0.2$, $\omega=7.7$, and using $N=1000$ terms in the sum.

Another example of "localization of singularities" is provided by the function

$$f_s(x)=\sum_{n=1}^{\infty} n^{-m-(1/2)}e^{i\omega \ln(\omega n)}x^{-s_n}. \tag{65}$$

Figure 4 shows this function $f_s(x)$ defined by Eq. (65) with $m=0.2,\omega=7.7$. One can observe a log-periodic set of structures, each structure composed of log-periodic oscillations converging to singular points beyond which damped oscillation can be observed. Here, the phase $\psi_n=\omega\ln(\omega n)$ is not varying fast enough with n to scramble the complex power laws x^{-s_n}, except at isolated points.

Figure 5 shows the graph of

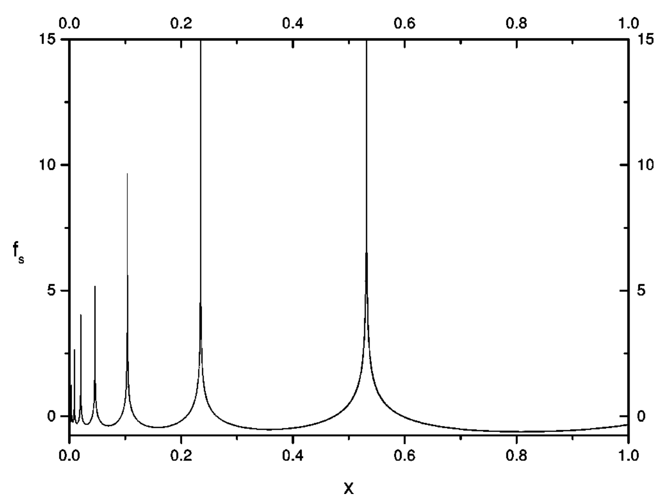

FIG. 5. Graph of $f_s(x)$ defined by Eq. (66) with $\psi_n=\omega n$, $m=0.2$, $\omega=7.7$, and with $N=1000$ terms in the sum.

$$f_s(x)=\sum_{n=1}^{\infty} n^{-m-(1/2)}e^{i\omega n}x^{-s_n}, \tag{66}$$

with $m=0.2, \omega=7.7$, and phases $\psi_n=\omega n$. Again, the phases are not sufficiently random to make the function irregular, except at isolated points where the constructive interference of the phases lead to the isolated singularities.

Note that both functions (65) and (66) can be analyzed with the method of Appendix B to obtain the functional form of the singularities.

2. Mixing phases

In contrast to the previous examples where the phases ψ_n are too regular, let us now take

$$\psi_n^{(0)}=\omega n\ln(\omega n) \tag{67}$$

corresponding to the asymptotic dependence (60) of the amplitudes A_n of the Weierstrass function. The phases (67) are ergodic and mixing on the unit circle. The corresponding function is

$$S(x)=\sum_{n=1}^{\infty} n^{-m-(1/2)}e^{i\omega n\ln(\omega n)}x^{-s_n}, \tag{68}$$

which we call the "log-periodic Weierstrass" function to stress the fact that it is constructed by summing log-periodic power laws x^{-s_n} [see for instance expression (37)] with amplitudes determined by the asymptotic behavior of the amplitudes of the power expansion of the Weierstrass function itself. The exponents s_n are again determined by Eq. (15) with m given by Eq. (8). By constructing Eq. (68), we are stripping off the Weierstrass function of its regular part and of all features that are unrelated to its fundamental nondifferentiability and self-affine properties. The definition of this "log-periodic Weierstrass" function (68) and its many generalizations studied below exemplifies the construction developed here. $S(x)$ exhibits the same nondifferentiability as does the Weierstrass function. In all these cases, $S(x)$ is nondifferentiable since $p=m+\frac{1}{2}<\frac{3}{2}$, in agreement with the conjecture of Sec. IV A.

Consider the general case

$$S_i(x)=\sum_{n=1}^{\infty} n^{-m-(1/2)}\exp(i\psi_n^{(i)})x^{-s_n}. \tag{69}$$

As other examples, let us now take

$$\psi_n^{(1)}=\omega n^2 \tag{70}$$

and

$$\psi_n^{(2)}=\omega e^{n/\omega}, \tag{71}$$

and form the corresponding sums for $i=1$ and 2. $\psi_n^{(0)}$, $\psi_n^{(1)}$, and $\psi_n^{(2)}$ cause similar irregular oscillations of $\cos[\psi_n^{(i)}]$ between -1 and $+1$ as a function of n, allowing for a nontrivial and complex interactions of singularities whose amplitudes (most important as we have seen) exhibit a slow power-law decay. As a result $S_1(x)$ and $S_2(x)$ exhibit very clear nondifferentiable features shown in Figs. 6 and 7.

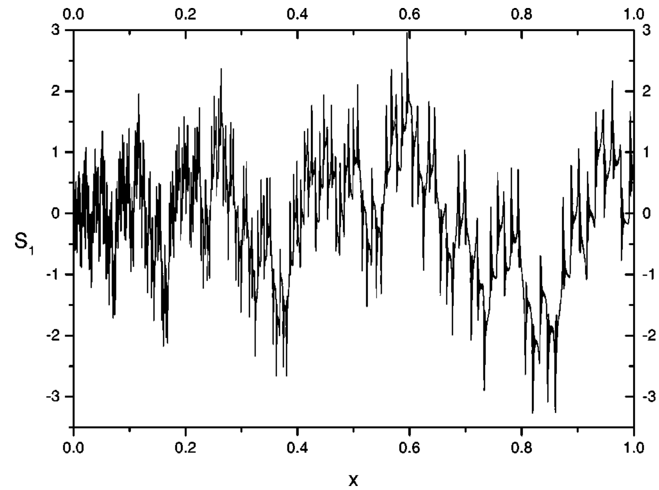

FIG. 6. Graph of $S_1(x)$ defined by Eq. (69) for the phases $\psi_n^{(1)}$ defined by Eq. (70) with $m=0.25, \omega=7.7, N=1000$.

Another very simple example of an ergodic phase is the quadratic rotator with irrational rotation number $0<R<1$,

$$\psi_{n+1}^{(3)}=\psi_n^{(3)}+2\pi Rn. \tag{72}$$

The most irregular phase is obtained for $R=g=(\sqrt{5}-1)/2=0.618\,033\,988\,75\ldots$, which is the Golden mean whose main property is that it is the least-well approximated by a rational number. The corresponding "Golden-mean log-periodic Weierstrass function" $S_3^{(g)}(x)$ defined by Eq. (69) with Eq. (72) is shown in Fig. 8. Other examples with $R=\pi/4=0.785\,398\,163\ldots$ and $R=1/e=0.367\,879\,441\ldots$ lead to $S_3^{(\pi/4)}(x)$ and $S_3^{(1/e)}(x)$ shown in Figs. 9 and 10. To each irrational number R corresponds an interesting Weierstrass-type functions whose delicately corrugated self-affine structure is encoded in the number-theoretical properties of its corresponding irrational number R.

Note that if Eq. (72) is changed to $\psi_{n+1}^{(3)}=\psi_n^{(3)}+2\pi R$, the corresponding observable $f(x)$ becomes smooth almost

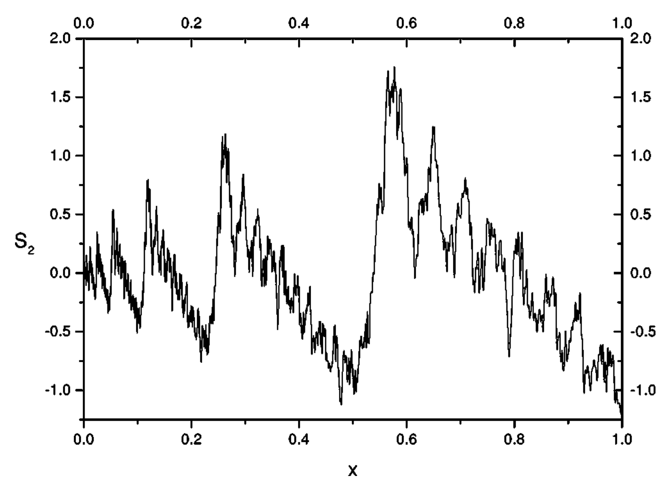

FIG. 7. Graph of $S_2(x)$ defined by Eq. (69) for the phases $\psi_n^{(2)}$ defined by Eq. (71) with $m=0.5, \omega=8, N=200$.

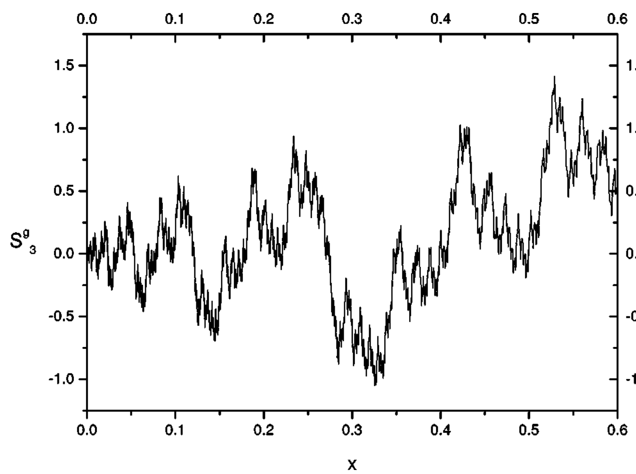

FIG. 8. "Golden-mean log-periodic Weierstrass function" $S_3^{(g)}(x)$ defined by Eq. (69) with Eq. (72) for $m=0.5,\omega=7.7,N=500$.

everywhere except at isolated points (also organized according to a geometrical series as described in Appendix B). The ergodic but nonmixing properties of the linear rotation map does not scramble the phases sufficiently to create nondifferentiability.

V. ILLUSTRATION OF THE CLASSIFICATION

Different physical problems will be encoded by different regular parts $g(x)$ quantifying the impact on the observable $f(x)$ of the degrees of freedom summed over two successive magnifications with the ratio λ. For a given physical problem, we perform the Mellin transform of $g(x)$. Then, together with the renormalization group structure (2), its formal solution (3), and its expansion (4) close to the leading critical point $x=0$ leading to Weierstrass-type functions, the classification (21) of the preceding section allows us to characterize the possible nondifferentiability and scaling properties of the observable $f(x)$.

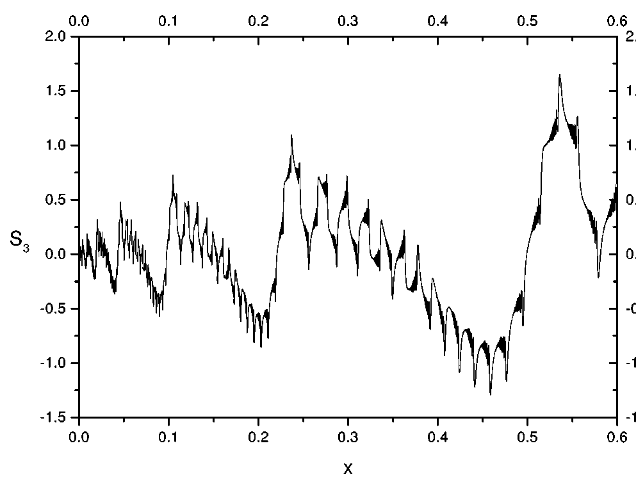

FIG. 9. "$\pi/4$-log-periodic Weierstrass function" $S_3^{(\pi/4)}$ defined by Eq. (69) with Eq. (72) and $R=\pi/4$ for $m=0.5,\omega=7.7,N=500$.

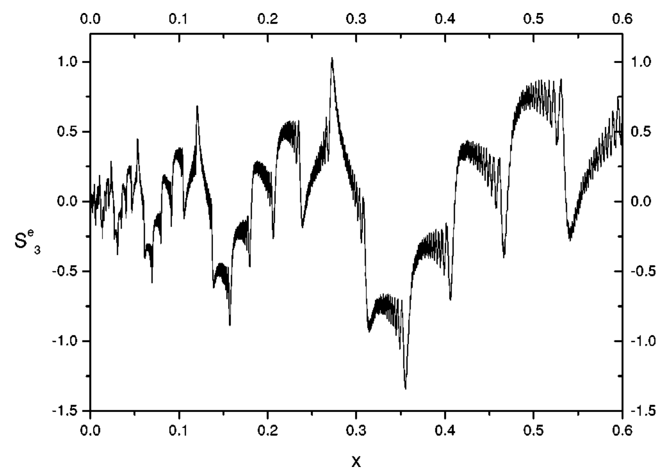

FIG. 10. "e-log-periodic Weierstrass function" $S_3^{(e)}$ defined by Eq. (69) with Eq. (72) and $R=e=2.718\ldots$ for $m=0.5,\omega=7.7,N=500$.

A. Other examples of the C^∞ differentiable family $\kappa>0$

For a general statistical mechanics model, the regular part $g(x)$ of the free energy has generally the form of the logarithm of a polynomial in x. Factorizing the polynomial, we do not lose generality by considering $g(x)$ given by

$$g(x)=\ln(1+x), \tag{73}$$

for which

$$\hat{g}(s)=\frac{\pi}{s\sin s\pi}. \tag{74}$$

The poles of $\hat{g}$ occur for $s=-n$, $n>0$, and contribute as already described only to the regular part of $f(x)$. Therefore, the Mellin transform of $f(x)$ is

$$\hat{f}(s)=\frac{\mu\gamma^s}{\mu\gamma^s-1}\frac{\pi}{s\sin(s\pi)}. \tag{75}$$

The regular part, determined by the poles at $s=-n$, $n>0$, reads

$$f_r(x)=\sum_{m=1}^{\infty}B(m)x^m,\quad B(m)=\frac{(-1)^{m+1}}{m}\frac{\mu}{\mu-\gamma^m}. \tag{76}$$

Note that constant term is absent. The singular part is

$$f_s(x)=\sum_{n=0}^{\infty}A_n x^{-s_n},\quad A_n=\frac{\pi}{\ln\gamma}\frac{1}{\sin(\pi s_n)s_n}. \tag{77}$$

The coefficients A_n converge to zero extremely fast for large n

$$A_n\sim\frac{1}{n}e^{-\pi\omega n}e^{-i\pi m},\quad n\to\infty, \tag{78}$$

where ω is given by Eq. (28). This corresponds to $p=1$, $\kappa=\pi\omega$, and $\psi_n=-\pi m$ in the general classification (21).

For the "Lorentzian,"

$$g(x)=(1+x^2)^{-1}, \tag{79}$$

the coefficients A_n of the power-law expansion (76) of the singular part $f_s(x)$ are

$$A_n=\frac{\pi}{2\ln\gamma}\frac{1}{\sin(\pi/2s_n)}, \tag{80}$$

with an asymptotic behavior given by

$$A_n\sim e^{-(\pi/2)\omega n}e^{i(\pi/2)m}, \quad n\to\infty. \tag{81}$$

This corresponds to $p=0$, $\kappa=(\pi/2)\omega$, and $\psi_n=\pi/2m$ in the general classification (21). The exponential decay rate $(\pi/2)\omega$ in this Lorentzian case is half that for the logarithm function (73). Both lead to C^∞ differentiable functions with extremely small amplitudes of log-periodic oscillations (see Table I).

For so-called stretched-exponential functions

$$g(x)=e^{-x^h}, \quad h>0, \tag{82}$$

we obtain

$$A_n(h)=\frac{\Gamma(s_n/h)}{\ln(\gamma)h}, \tag{83}$$

and

$$A_n(h)\sim\frac{1}{n^{m/h+1/2}}\exp\left[-\frac{\pi\omega}{2h}n\right]\exp\left[i\frac{\omega n}{h}\ln(\omega n)\right], \quad n\to\infty. \tag{84}$$

Log-periodic stretched-exponential function $f_s(x,h)$ and all its derivatives (on x) converge. This corresponds to $p=(m/h)+(1/2)$, $\kappa=(\pi/2)(\omega/h)$, and $\psi_n=(\omega n/h)\ln(\omega n)$ in the general classification (21). Since $\kappa>0$, the corresponding singular function $f_s(x)$ is differentiable at all orders. However, a limit of nondifferentiability at isolated points can be reached formally by taking the limit $h\to\infty$ for which $p\to 1/2$, $\kappa\to 0^+$, and $\psi_n\to 0$. Then, $f_s(x)$ exhibits the nondifferentiability at points x_u verifying $x_u=1/\gamma^u$ defined in Eq. (B1) studied in Sec. IV D 1. This is shown in Figs. 11 with the dependence of $f_s(x,h)$ on the parameter h. As h increases, $g(x)$ becomes more-and-more localized close to the origin and $f_s(x)$ exhibits more-and-more pronounced steps. Formally, the limit $h\to\infty$ allows us to crossover from the class $\kappa>0$ to the class $\kappa=0$.

B. Other examples of the Weierstrass-type function class $\kappa=0$

We have noted above that a nondifferentiable function is everywhere oscillating and the length of arc between any two points on the curve is infinite [21]. Its regular generator $g(x)$ must thus contain oscillations or must exhibit at least compact support (so that it has a discrete Fourier series) in order for $f(x)$ to be nondifferentiable or for some of its derivatives to be nondifferentiable. We illustrate this remark by several examples.

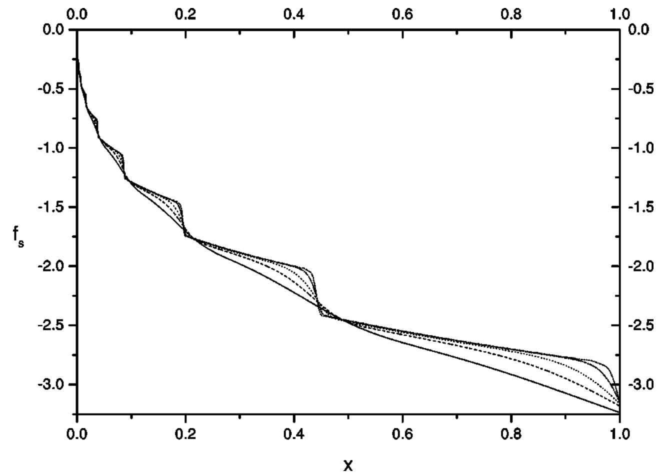

FIG. 11. Singular part $f_s(x)$ of the Weierstrass-like function for the regular function $g(x)$ equal to the stretched exponential (82) for $h=5$ (solid line), $h=10$ (dashed line), $h=20$ (dotted line), $h=50$ (dashed-dotted line), and $h=100$ (dashed-dot-dotted line), for $m=0.4,\omega=7.7,N=22$.

1. Generalized periodic processes

Let us consider the function generalizing the sine function by taking an arbitrary real exponent δ,

$$g(x)=\frac{\sin(x)}{x^\delta}. \tag{85}$$

The Weierstrass function is recovered for $\delta=0$. The coefficients A_n of the expansion in power series of the singular part can be obtained by a simple shift of s in the expression obtained for the Weierstrass function

$$A_n(\delta)=\frac{\Gamma(s_n-\delta)\sin\left[\frac{1}{2}\pi(s_n-\delta)\right]}{\ln\gamma}. \tag{86}$$

For $m+\delta\leqslant 1$, the log-periodic generalized sine function $f_s(x,\delta)$ as well as its associated Weierstrass-type function are continuous but nondifferentiable.

The asymptotic behavior of the coefficient A_n is

$$A_n(\delta)\sim n^{-m-\delta-1/2}\exp[-i\omega n\ln(\omega n)], \quad n\to\infty. \tag{87}$$

This corresponds to $p=m+\delta+1/2$, $\kappa=0$, and $\psi_n=\omega n\ln(\omega n)$ in the general classification (21). Figure 12 shows the generalized sine function $f_s(x,\delta)$ for different values of δ for $\delta=-0.1$ (solid line), $\delta=0$ (dashed line), and $\delta=0.1$ (dotted line) for $m=0.4$ and $\omega=7.7$.

Another interesting case is the sine integral, $g(x)=Si(x)\equiv\int_0^x dv[(\sin v)/v]$. The coefficients A_n of the power-law series of the singular part are given by

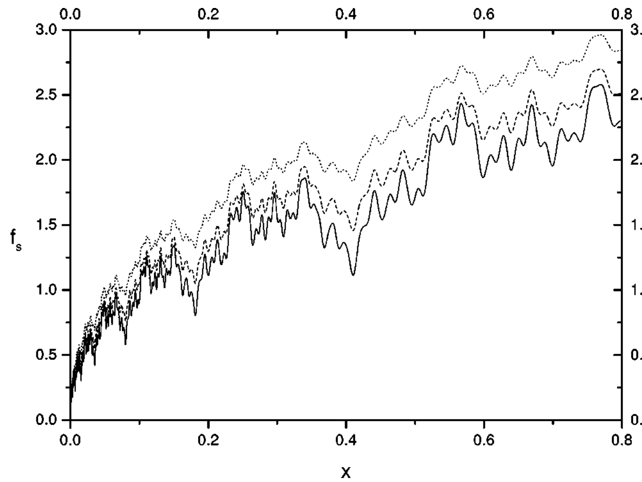

FIG. 12. Singular part $f_s(x,\delta)$ of the Weierstrass-like function for the regular function $g(x)$ given by Eq. (85) for $\delta=-0.1$ (solid line), $\delta=0$ (dashed line), and $\delta=0.1$ (dotted line) for $m=0.4,\omega=7.7,N=27$).

$$A_n=-\frac{\Gamma(s_n)\sin\left(\frac{1}{2}\pi s_n\right)}{s_n\ln\gamma},\qquad(88)$$

with asymptotics

$$A_n\sim n^{-m-3/2}\exp\left[-i\omega n\ln(\omega n)+\frac{\pi}{2}m\right],\quad n\to\infty,\qquad(89)$$

corresponding to $p=m+3/2$, $\kappa=0$, and $\psi_n=\omega n\ln(\omega n)+(\pi/2)m$ in the general classification (21). All three functions $f(x)$, $f_s(x)$, and $S(x)$ defined by Eq. (68) have a continuous but nondifferentiable first derivative for $m<1$. However, the delicate log-periodic corrugations are enhanced in the graph of $S(x)$.

2. Localized processes

Let us now study functions $g(x)$ with compact support such as

$$g(x)=(1-x^h)^{\nu-1},\quad 0\leqslant x\leqslant 1,\quad g(x)=0$$
$$\text{for } x>1 \text{ with } h\geqslant 1 \text{ and } \nu\geqslant 2.\qquad(90)$$

The coefficients A_n of the power series expansion of the singular part $F_s(x)$ are

$$A_n(\nu,h)=\frac{B(\nu,s_n/h)}{\ln(\gamma)h},\qquad(91)$$

where $B(x,y)=[\Gamma(x)\Gamma(y)]/[\Gamma(x+y)]$ is the β function. Figure 13 shows the function $f(x)$ obtained from the direct sum (4). Figure 14 shows how the shape of the log-periodical structures steepen with increasing h, as the function $g(x)$ evolves from a half-$\cap$ shape to the plateau $g(0<x<1)=1$ and 0 otherwise. The log-periodic geometrical series of plateaux and steps shown in Fig. 14 is reminiscent of the structures found for rupture [5,28,29] and earthquakes [6,30] precursors.

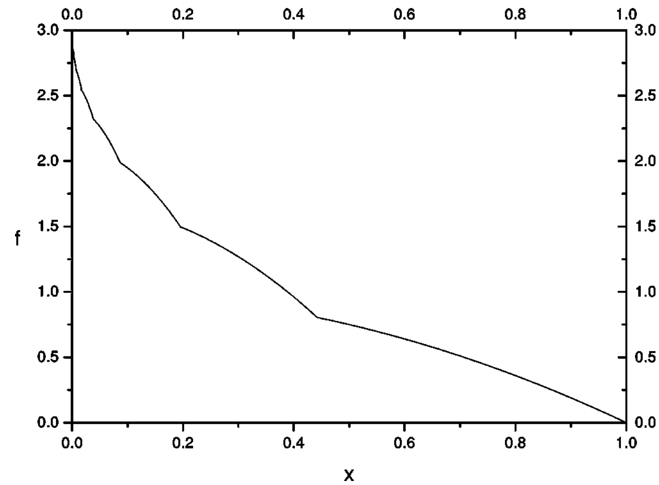

FIG. 13. Weierstrass-type function $f(x)$ for compact $g(x)$ given by Eq. (90) with $\nu=2,h=2$ for $m=0.5,\omega=7.7,N=47$.

The asymptotic behavior of $A_n(\nu)$ is

$$A_n(\nu,h)\sim\frac{e^{i\pi}}{n^{\nu}},\quad\text{with } \nu\geqslant 2,\quad n\to\infty,\qquad(92)$$

corresponding to $p=\nu$, $\kappa=0$, and $\psi_n=\pi$ in the general classification (21).

As the phases $\psi_n=\pi$ are constant and their contribution can be factorized, the function $f_s(x,\nu)$ has a behavior similar to the function (62) analyzed in Sec. IV D 1. In particular, we recover the fact that the points $x_u=1/\gamma^u$ given by Eq. (B1) make the imaginary contribution of x^{-s_n} vanish. As a consequence, they are the most singular points. An analysis similar to that presented in Sec. IV D 1 can be performed.

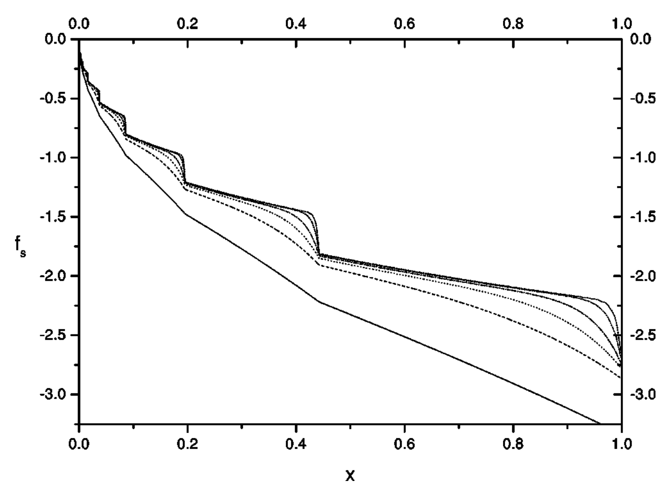

FIG. 14. Evolution of the "singular part" $f_s(x)$ corresponding to the compact regular part $g(x)$, Eq. (90) for $\nu=2$ with increasing abruptness of $g(x)$ quantified by the exponent h: $h=2$ (solid), $h=5$ (dash), $h=10$ (dot), $h=20$ (dash dot), $h=50$ (dash-dot-dot), $h=100$ (short dash), for $m=0.5,\omega=7.7,N=47$.

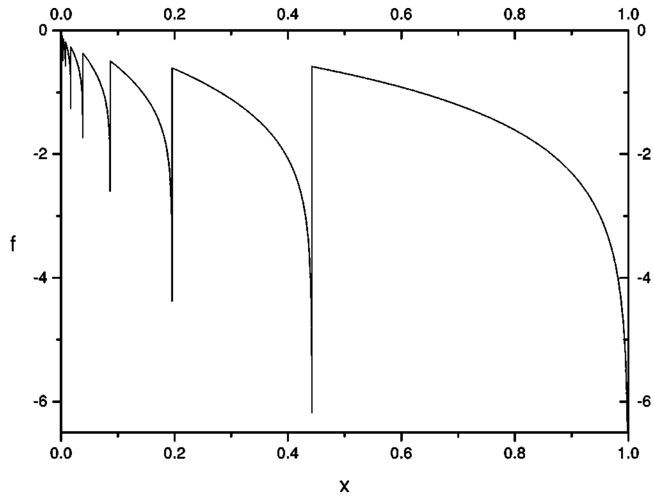

FIG. 15. Weierstrass-type function $f(x)$ corresponding to the regular part $g(x)$ defined by Eq. (93) with compact support, with $m=0.5,\omega=7.7,N=47$.

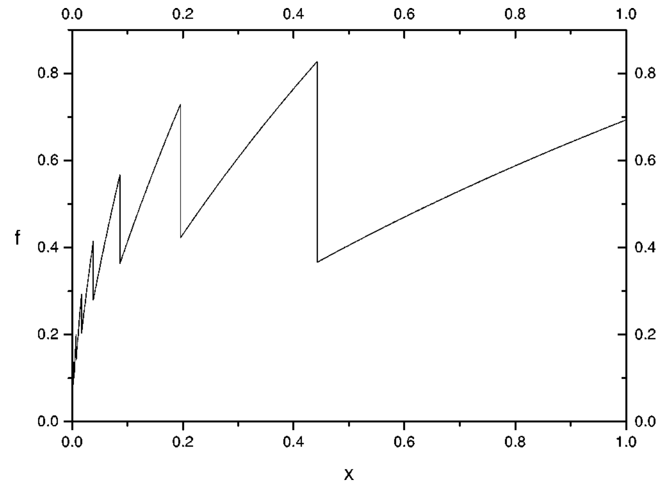

FIG. 16. Weierstrass-type function $f(x)$ corresponding to the regular part $g(x)$ defined by Eq. (96) with compact support, with $m=0.5,\omega=7.7,N=47$.

Another example corresponds to the logarithmic function

$$g(x)=\ln(1-x),\quad 0<x<1 \quad \text{and} \quad g(x)=0 \quad \text{for} \quad x>1, \tag{93}$$

with compact support. Figure 15 shows the corresponding Weierstrass function $(m=0.5,\omega=7.7,N=47)$. The coefficients in the power expansion are given by

$$A_n=-\frac{1}{s_n}[\Psi(1+s_n)-\Psi(1)], \tag{94}$$

where Ψ is the logarithmic derivative of the Γ function.

The asymptotic behavior of the coefficients A_n is

$$A_n\sim\frac{\ln(n)}{n}\exp\left[i\left\{-\arctan\left(\frac{2\ln(\omega n)}{\pi}\right)+\pi\right\}\right],\quad (n\to\infty), \tag{95}$$

corresponding to $p=1$, $\kappa=0$, and $\psi_n=\arctan\{[2\ln(\omega n)]/\pi\}$ in the general classification (21). The logarithmic "correction" to the power law $1/n$ comes from the singularity at $x=1$. This example illustrates a possible cause for a deviation from the classification (21). Such modification, however, does not change the qualitative picture as they correspond to the next subdominant correction to the power-law contribution to A_n.

The relative amplitudes of the two first power-law terms are given by $|A_{n=1}/A_{n=0}|=0.143$, $|A_{n=2}/A_{n=0}|=0.086$, $(m=0.5,\omega=7.7)$.

For the nonsingular compact logarithmic regular part

$$g(x)=\ln(1+x),\quad 0<x<1 \quad \text{and} \quad g(x)=0 \quad \text{for} \quad x>1, \tag{96}$$

Fig. 16 shows the corresponding Weierstrass-type function $f(x)$. The coefficients in the power series expansion are

$$A_n=\frac{1}{s_n}\left[\ln 2-\frac{1}{2}\Psi\left(1+\frac{s_n}{2}\right)+\frac{1}{2}\Psi\left(\frac{1}{2}+\frac{s_n}{2}\right)\right], \tag{97}$$

where Ψ is again the logarithmic derivative of the Γ function. The asymptotic behavior of the coefficients A_n is

$$A_n\sim\frac{1}{n}\exp\left[i\left(\arctan\left(\frac{\omega n}{m}\right)+\pi\right)\right],\quad (n\to\infty), \tag{98}$$

corresponding to $p=1$, $\kappa=0$, and $\psi_n=\arctan([\omega n/m])+\pi$ in the general classification (21). The relative amplitudes of the two first power-law terms are given by $|A_{n=1}/A_{n=0}|=0.016$, $|A_{n=2}/A_{n=0}|=7.738\times10^{-3}$ for $m=0.5,\omega=7.7$. Thus, even if the asymptotic decay is almost the same as for Eq. (93) up to the logarithmic correction, the log-periodic amplitudes of the leading terms are a factor of 10 smaller.

VI. DISCUSSION

This paper has studied the solutions of Eq. (4), which can be understood as a renormalization group equation with a single control parameter or more generally as the Jackson q integral describing discrete-scale-invariant systems. We have emphases on the factors controlling the presence and amplitude of log-periodic corrections to the leading power-law solution. We have used the Mellin transform to resum the formal series solution of the DSI equation into a power-law series and have presented a general classification within two classes

(1) Systems with quasiperiodic "regular part" and/or with compact support present strong log-periodic oscillatory amplitudes.

(2) Systems with nonperiodic "regular part" with unbound support have exceedingly small log-periodic oscillatory amplitudes and regular smooth observables.

In systems for which the renormalization group equation has been explicited, systems of the first class are associated with "antiferromagnetic" interactions. Systems of the second class occur when the microscopic interactions are dominantly "ferromagnetic."

We hope to quantify in future works how these facts may help interpret the observation of strong log-periodic oscillations in out-of-equilibrium growth processes, rupture, earthquakes, and in finance. Our analysis of its impact on the "regular part" $g(x)$ of the DSI equation shows that $g(x)$ plays a key role and may record the nature of interactions that lead to its different classes of behavior. However, determining the observables that take the place of the equilibrium free energy for growth models that could be obtained recursively (via a renormalization group transformation), or equivalently, the identification of the meaning of the function $g(x)$, remains an unsolved problem in general (see, however, the iterative conformal mapping used in the theory of diffusion-limited aggregation, which provides a scaling function for DLA [45]).

ACKNOWLEDGMENT

We are grateful to A. Erzan for a discussion on Jackson's integral and for supplying the corresponding references.

APPENDIX A: DIFFERENTIABILITY PROPERTIES OF THE "LOCALIZATION OF SINGULARITIES"

Using the asymptotic expression (63), we can write

$$\mathrm{Re}[\overline{f_s(x)}]=G(x)+x^m\sum_{n=n_r}^{\infty}\frac{1}{n^{m+1/2}}\cos\left(2\pi n\frac{\ln x}{\ln\gamma}\right), \tag{A1}$$

where $G(x)=\Sigma_{n=0}^{n_r}|A_n(\pi/2)|x^{-s_n}$ is a regular function. $\mathrm{Re}[\overline{f_s(x)}]$ denotes the real part of $\overline{f_s(x)}$ and we have used Eq. (15). The second term of the r.h.s. of Eq. (A1), which can be called the singular part of $\mathrm{Re}[\overline{f_s(x)}]$ and is denoted $G_s(x)$, is a sum starting at an index n_r that is taken sufficiently large such that the asymptotic expression (63) holds to within any desired degree of accuracy.

The singular part $G_s(x)$ has the same analytical behavior as the function

$$K_p(y)\equiv\sum_{n=1}^{\infty}\frac{1}{n^p}\cos(ny),\quad p=m+\frac{1}{2}, \tag{A2}$$

where $y=2\pi\ln x/\ln\gamma$. This function is a special case of $K_{p,\{\psi_n\}}(y)$ defined by Eq. (41) for $\psi_n=0$.

This function $K_p(y)$ has been studied in the literature for special cases. When the real part of p is larger than 1, the sum is absolutely convergent for all x. Restricting our attention to real exponents p, the series $K_p(y=\pi)=-\Sigma_{n=1}^{\infty}[(-1)^{n+1}/n^p]$, which corresponds to $y=(2\ell+1)\pi$ where ℓ is an arbitrary integer, is convergent for all positive p to $K_p(y=\pi)=(1-2^{1-p})\zeta(p)$ [40], where $\zeta(p)$ is the Riemann ζ function. Obviously, $K_p(y=2\pi)$ is infinite for $p<1$ and we show below that $K_p(y\to 2\pi)$ has a power-law singularity. For $p>1$, $K_p(y)$ can be expressed as

$$K_p(y)=\frac{(2\pi)^p}{4\Gamma(p)}\sec\left(\frac{\pi p}{2}\right)\left[\zeta\left(1-p,\frac{y}{2\pi}\right)-\zeta\left(1-p,1-\frac{y}{2\pi}\right)\right], \tag{A3}$$

where $\zeta(s,\nu)=\Sigma_{k=0}^{+\infty}[\nu+k]^{-s}$ is the generalized Riemann ζ function [44].

For $p>0$ and except for the special value $y=0$ modulus 2π, $K_p(y)$ is finite and differentiable. To see this, let us consider rational values of $y/2\pi=r/q$ with $q\geqslant 2$, where r/q is the irreducible representation of the rational $y/2\pi$. We can rearrange the series in Eq. (A2) into q subseries as follows:

$$\begin{aligned}K_p(y)&=\mathrm{Re}\left(\sum_{k=1}^{\infty}\frac{1}{(kq)^p}+\sum_{k=1}^{\infty}\frac{e^{i2\pi(q-1)(r/q)}}{(kq-1)^p}+\sum_{k=1}^{\infty}\frac{e^{i2\pi(q-2)(r/q)}}{(kq-2)^p}+\cdots+\sum_{k=1}^{\infty}\frac{e^{i2\pi 2(r/q)}}{(kq-q+2)^p}\right.\\&\left.\quad+\sum_{k=1}^{\infty}\frac{e^{i2\pi(r/q)}}{(kq-q+1)^p}\right)=\mathrm{Re}\sum_{j=1}^{q}\left(\sum_{k=0}^{\infty}\frac{e^{i2\pi j(r/q)}}{(kq+j)^p}\right)\\&=\mathrm{Re}\sum_{k=0}^{\infty}\left(\sum_{j=1}^{q}\frac{e^{i2\pi j(r/q)}}{(kq+j)^p}\right).\end{aligned} \tag{A4}$$

We expand

$$1/(kq+j)^p=(kq)^{-p}\left[1-\frac{p}{kq}j+\frac{p(p+1)}{2}\frac{j^2}{(kq)^2}+\cdots\right]$$

and get

$$\begin{aligned}K_p(y/2\pi=r/q)&=\mathrm{Re}\sum_{k=0}^{\infty}\frac{1}{(kq)^p}\left(\sum_{j=1}^{q}e^{i2\pi j(r/q)}-\frac{p}{kq}\sum_{j=1}^{q}je^{i2\pi j(r/q)}+\frac{p(p+1)}{2(kq)^2}\right.\\&\left.\quad\times\sum_{j=1}^{q}j^2e^{i2\pi j(r/q)}+\cdots\right).\end{aligned} \tag{A5}$$

Calling w_q the qth root of 1, i.e., $w_q=e^{i2\pi/q}$, we have then $w_q+w_q^2+\cdots+w_q^{q-1}+w_q^q=(1-w_q^q)/(1-w)=0$. Hence, the first sum $\Sigma_{j=1}^{q}e^{i2\pi j(r/q)}$ in Eq. (A5) is identically zero. The other sums are nonzero and finite. We thus get

$$K_p(y/2\pi=r/q)=\sum_{k=0}^{\infty}\frac{C_k(r,q)}{k^{p+1}}, \tag{A6}$$

where

$$C_k(r,q)=\frac{1}{q^{p+1}}\mathrm{Re}\left[\sum_{j=1}^{q}e^{i2\pi j(r/q)}\left(-pj+\frac{p(p+1)}{2(kq)}j^2-\frac{p(p+1)(p+2)}{6(kq)^2}j^3+\cdots\right)\right] \tag{A7}$$

is bounded from above as $k\to+\infty$. The expression (A6) shows that $K_p(y/2\pi=r/q)$ is finite for any $p>0$. Now, since rational numbers are dense among real numbers, i.e., any irrational number can be approached arbitrarily close by a rational number, by the condition of continuity, $K_p(y)$ is finite everywhere, except for $y/2\pi = r/q$ with $q=1$. Differentiating the expression (A2) gives the series $\Sigma_{n=1}^{\infty}(1/n^{p-1})\sin(ny)$. By the same reasoning leading to Eq. (A6), this derivative is bounded from above by a constant times $\Sigma_{n=1}^{\infty}(1/n^{p})$ that is convergent for $p>1$. This shows that $K_p(y)$ is differentiable for $p>1$, and thus $\mathrm{Re}[\overline{f_s(x)}]$ is differentiable for $m>1/2$. This approach is not powerful enough, however, to treat the case $m<1/2$.

APPENDIX B: FUNCTIONAL SHAPE OF THE DENUMERABLE SET OF DISCRETE SINGULARITIES RESULTING FROM THE "LOCALIZATION OF SINGULARITIES"

We now examine the special case $y/2\pi = r/q$ with $q=1$. From the expression (A1), the values x_u, which are such that $\ln x_u/\ln\gamma$ is an integer $-u$, i.e.,

$$x_u = 1/\gamma^u, \tag{B1}$$

make all the cosine terms in the infinite sum in phase and equal to 1. Thus,

$$G_s(x_u) = x^m \sum_{n=n_r}^{\infty} \frac{1}{n^{m+(1/2)}}, \tag{B2}$$

which diverges for $m \leq 1/2$. At the border case $m=1/2$, the divergence is logarithmic. Similarly, $dG_s/dx|_{x=x_u}$ diverges for $m<3/2$ as an additional power of n is brought to each term in the sum by taking the derivative. This and expression (B1) explain the graphs of Fig. 3.

The functional shapes of the spikes for $x \to x_u$ can be determined as follows. For $x \to x_u$,

$$\cos\left(2\pi n \frac{\ln x}{\ln\gamma}\right) = \cos\left(\frac{2\pi n\epsilon}{\ln\gamma}\right) + O(\epsilon^2),$$

where $\epsilon \equiv (x-x_u)/x_u$ and $O(\epsilon^2)$ represents a term proportional to ϵ^2. Let us now construct and compare $G_s(\epsilon)$ and $G_s(\lambda\epsilon)$, where λ is an arbitrary number. Up to first order in ϵ, we have

$$G_s(\lambda\epsilon) \approx x_u^m \sum_{n=n_r}^{\infty} \frac{\cos\left(\frac{2\pi n\lambda\epsilon}{\ln\gamma}\right)}{n^{m+1/2}}. \tag{B3}$$

Posing $n' = \mathrm{Int}(n\lambda)$, $G_s(\lambda\epsilon)$ can be rewritten

$$G_s(\lambda\epsilon) \approx x_u^m \sum_{n'=\mathrm{Int}[n_r\lambda]}^{\infty} \frac{\lambda^{m+(1/2)}}{\lambda} \frac{\cos\left(\frac{2\pi n'\epsilon}{\ln\gamma}\right)}{n'^{m+(1/2)}}$$

$$= x_u^m \lambda^{m-(1/2)} \sum_{n'=\mathrm{Int}[n_r\lambda]}^{\infty} \frac{\cos\left(\frac{2\pi n'\epsilon}{\ln\gamma}\right)}{n'^{m+(1/2)}}. \tag{B4}$$

Note the presence of the additional multiplicative term $\lambda^{m+(1/2)/\lambda}$ in the sum of (B4). The numerator $\lambda^{m+(1/2)}$ stems from replacing n by $n' = \mathrm{Int}(n\lambda)$ in $1/n^{m+(1/2)}$. The other factor $1/\lambda$ is the "Jacobian" of the change from n to $n' = \mathrm{Int}(n\lambda)$. Expression (B4) can then be rewritten as

$$G_s(\lambda\epsilon) \approx \lambda^{m-(1/2)} G_s(\epsilon) + H_r(\epsilon), \tag{B5}$$

where

$$H(\epsilon) = \lambda^{m-(1/2)} \sum_{n=n_r}^{\mathrm{Int}[n_r\lambda]-1} \frac{\cos\left(\frac{2\pi n'\epsilon}{\ln\gamma}\right)}{n'^{m+(1/2)}} \tag{B6}$$

is a regular function of ϵ. The singular part of $G_s(\epsilon)$ is solution of $G_s(\lambda\epsilon) \approx \lambda^{m-(1/2)} G_s(\epsilon)$, i.e.,

$$G_s(\epsilon) \sim \epsilon^{m-(1/2)}. \tag{B7}$$

This confirms that, for $0<m<1/2$ (panel *a* of Fig. 3), the spikes correspond to a divergence of $G_s(x)$ as $x \to x_u$ according to $G_s(x) \sim 1/|x-x_u|^{(1/2)-m}$. For $1/2<m<3/2$, $G_s(x)$ goes to a finite value as $x \to x_u$ but with an infinite slope (since $0<m-\frac{1}{2}<1$) according to $G_s(x) \sim \mathrm{constant} - |x - x_u|^{m-(1/2)}$. The borderline case $m=1/2$ can actually be summed exactly as $K_{p=1}(y) = -\frac{1}{2}\ln(2[1-\cos y])$ [40]. When $y \to 0$ modulo 2π, $K_{p=1}(y)$ diverges as $\ln(1/y)$ and thus $G_s(\epsilon)$ diverges as $G_s(\epsilon) \sim \ln|x_u/(x-x_u)|$.

[1] D. Sornette, Phys. Rep. **297**, 239 (1998).
[2] B. Derrida, C. Itzykson, and J. M. Luck, Commun. Math. Phys. **94**, 115 (1984).
[3] D. Sornette, A. Johansen, A. Arnéodo, J.-F. Muzy, and H. Saleur, Phys. Rev. Lett. **76**, 251 (1996).
[4] Y. Huang, G. Ouillon, H. Saleur, and D. Sornette, Phys. Rev. E **55**, 6433 (1997).
[5] A. Johansen and D. Sornette, Eur. Phys. J. B **18**, 163 (2000).
[6] D. Sornette and C. G. Sammis, J. Phys. I **5**, 607 (1995).
[7] D. Sornette, A. Johansen, and J.-P. Bouchaud, J. Phys. I **6**, 167 (1996).
[8] A. Johansen, D. Sornette, and O. Ledoit, J. Risk **1**, 5 (1999).
[9] F. H. Jackson, Q. J. Pure. Appl. Math. **41**, 193 (1910); Q. J. Math. **2**, 1 (1951).
[10] A. Erzan, Phys. Lett. A **225**, 235 (1997).
[11] A. Erzan and J.-P. Eckmann, Phys. Rev. Lett. **78**, 3245 (1997).
[12] B. Derrida, J.-P. Eckmann, and A. Erzan, J. Phys. A **16**, 893 (1983).
[13] S. R. McKay, A. N. Berker, and S. Kirkpatrick, Phys. Rev. Lett. **48**, 767 (1982).
[14] G. Paul, Phys. Rev. E **59**, 4847 (1999).
[15] *Scale Invariance and Beyond*, edited by B. Dubrulle, F. Graner, and D. Sornette (EDP Sciences and Springer, Berlin, 1997).

[16] D. Sornette, *Critical Phenomena in Natural Sciences*, Springer Series in Synergetics (Springer, Berlin, 2000).
[17] N. Goldenfeld, *Lectures on Phase Transitions and the Renormalization Group* (Addison-Wesley, Reading, MA, 1992).
[18] A. Erzan, Phys. Lett. A **225**, 235 (1997).
[19] K. Weierstrass, in *Classics on Fractals*, edited by G. A. Edgar (Addison-Wesley, Reading, MA, 1993), pp. 3–9.
[20] G. H. Hardy, Trans. Am. Math. Soc. **17**, 301 (1916).
[21] A. N. Singh, *Squaring the Circle and Other Monographs* (Chelsea Publishing Company, New York, 1953).
[22] L. F. Richardson, Proc. R. Soc. London, Ser. A **110**, 709 (1926).
[23] B. D. Hughes, M. F. Shlesinger, and E. W. Montroll, Proc. Natl. Acad. Sci. U.S.A. **78**, 3287 (1981); E. W. Montroll and M. F. Shlesinger, in *Studies in Statistical Mechanics*, edited by J. Lebowitz and E. Montroll (North-Holland, Amsterdam, 1984), Vol. 11, p. 1; J. Klafter, M. F. Shlesinger, and G. Zumofen, Phys. Today **49**(2), 33 (1996); M. F. Shlesinger, G. M. Zaslavsky, and J. Klafter, Nature (London) **363**, 31 (1993).
[24] H. Saleur and D. Sornette, J. Phys. I **6**, 327 (1996).
[25] M. L. Lapidus and M. van Frankenuysen, *Fractal Geometry and Number Theory* (Birkhäuser, Boston, 2000).
[26] Yu. V. Sidorov, M. V. Fedoryuk, and M. I. Shabunin, *Lectures in Theory of Complex Variable*s (Nauka, Moscow, 1989), p. 480.
[27] F. Oberhettinger, *Tables of Mellin Transforms* (Springer-Verlag, New York, 1974), p. 275
[28] J.-C. Anifrani, C. Le Floc'h, D. Sornette, and B. Souillard, J. Phys. I **5**, 631 (1995).
[29] A. Johansen and D. Sornette, Int. J. Mod. Phys. C **9**, 433 (1998).
[30] H. Saleur, C. G. Sammis, and D. Sornette, J. Geophys. Res., [Solid Earth] **101**, 17 661 (1996).
[31] A. Johansen, H. Saleur, and D. Sornette, Eur. Phys. J. B **15**, 551 (2000).
[32] A. Johansen and D. Sornette, Eur. Phys. J. B **17**, 319 (2000).
[33] R. Metzler, J. Klafter, and J. Jortner, Proc. Natl. Acad. Sci. U.S.A. **96**, 11085 (1999).
[34] T.-Y. Hu and K.-S. Lau, Trans. Am. Math. Soc. **335**, 649 (1993).
[35] E. C. Titchmarsh, *The Zeta-Function of Riemann* (Cambridge University Press, London, 1930), p. 104.
[36] H. M. Edwards, *Riemann's Zeta Function* (Academic Press, New York, 1974).
[37] J. L. Kaplan, J. Mallet-Paret, and J. A. Yorke, Ergod. Theory Dyn. Syst. **4**, 261 (1984).
[38] *Tables of Integral Transforms*, edited by A. Erde'lyi (McGraw-Hill, New York, 1954).
[39] N. N. Lebedev, *Special Functions and their Applications* (Prentice-Hall, Englewood Cliffs, NJ, 1965), p. 308.
[40] I. S. Gradshteyn and I. M. Ryzhik, in *Table of Integrals, Series, and Products*, 4th ed., edited by Yu. V. Geronimus and M. Yu. Tseytlin, translated from the Russian by Scripta Technika, Inc. Translation edited by Alan Jeffrey (New York, Academic Press, 1965).
[41] M. V. Berry and Z. V. Lewis, Proc. R. Soc. London, Ser. A **370**, 459 (1980).
[42] B. R. Hunt, Proc. Am. Math. Soc. **126**, 791-800 (1998).
[43] B. Mandelbrot, *The Fractal Geometry of Nature* (Freeman, San Francisco, 1982).
[44] A. P. Prudnikov, Yu. A. Brychkov, and O. I. Marichev, *Integrals and Series*, translated from the Russian by N. M. Queen (Gordon and Breach Science Publishers, New York, 1992).
[45] B. Davidovitch, A. Levermann, and I. Procaccia, Phys. Rev. E **62**, R5919 (2000).